AD NUMBER

ADB032318

NEW LIMITATION CHANGE

TO

Approved for public release, distribution unlimited

FROM

Distribution authorized to U.S. Gov't. agencies only; Test and Evaluation; JUN 1978. Other requests shall be referred to Air Force Flight Dynamics Laboratory, Attn: FBR, Wright-Patterson AFB, OH 45433.

AUTHORITY

afwal ltr, 29 jul 1981

AFFDL-TR-78-116

LEVEL
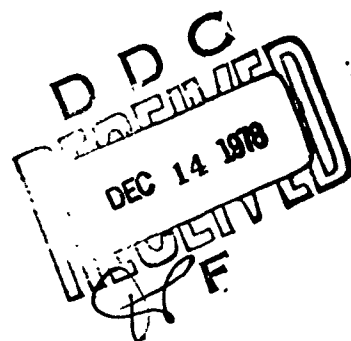
AEROELASTIC STABILITY AND PERFORMANCE CHARACTERISTICS OF AIRCRAFT WITH ADVANCED COMPOSITE SWEPTFORWARD WING STRUCTURES

Terrence A. Weisshaar

Virginia Polytechnic Institute and State University
Aerospace and Ocean Engineering Department
Blacksburg, Virginia 24061

DDC
DEC 14 1978
F

September 1978

FINAL REPORT FOR PERIOD SEPTEMBER 1977 - JUNE 1978

78 12 11 002

REPORT DOCUMENTATION PAGE

READ INSTRUCTIONS BEFORE COMPLETING FORM

1. REPORT NUMBER	2. GOVT ACCESSION NO.	3. RECIPIENT'S CATALOG NUMBER
AFFDL-TR-78-116		

4. TITLE (and Subtitle)

AEROELASTIC STABILITY AND PERFORMANCE CHARACTERISTICS OF AIRCRAFT WITH ADVANCED COMPOSITE SWEPTFORWARD WING STRUCTURES

5. TYPE OF REPORT & PERIOD COVERED

FINAL REPORT.
September 1977 — June 1978

6. PERFORMING ORG. REPORT NUMBER

7. AUTHOR(s)

Terrence A. Weisshaar

8. CONTRACT OR GRANT NUMBER(s)

AFOSR-77-3423

9. PERFORMING ORGANIZATION NAME AND ADDRESS

Virginia Polytechnic Institute & State University
Aerospace and Ocean Engineering Department
Blacksburg, Virginia 24061

10. PROGRAM ELEMENT, PROJECT, TASK AREA & WORK UNIT NUMBERS

PE: 62702E
DARPA Order No. 3436
Task: 343600

11. CONTROLLING OFFICE NAME AND ADDRESS

Air Force Flight Dynamics Laboratory (FBR)
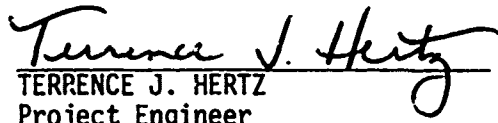Air Force Wright Aeronautical Laboratories (AFSC)
Wright-Patterson AFB, Ohio 45433

12. REPORT DATE

September 1978

13. NUMBER OF PAGES

56

14. MONITORING AGENCY NAME & ADDRESS(If different from Controlling Office)

66p.

15. SECURITY CLASS. (of this report)

Unclassified

15a. DECLASSIFICATION/DOWNGRADING SCHEDULE

16. DISTRIBUTION STATEMENT (of this Report)

Distribution limited to U.S. Government agencies only; test and evaluation; June 1978. Other requests for this document must be referred to the Air Force Flight Dynamics Laboratory (FBR), Wright-Patterson Air Force Base, Ohio 45433.

17. DISTRIBUTION STATEMENT (of the abstract entered in Block 20, if different from Report)

18. SUPPLEMENTARY NOTES

19. KEY WORDS (Continue on reverse side if necessary and identify by block number)

Aeroelastic Tailoring
Composites
Forward Swept Wings

20. ABSTRACT (Continue on reverse side if necessary and identify by block number)

Sweptforward metallic wings have not been considered to be a serious design concept for nearly thirty years. The large structural weights necessary to preclude aeroelastic divergence of metallic wing structures are unfavorable when compared to similar sweptback designs, designs that are usually divergence free. The development of fibrous laminated composite materials and the fact that forward swept wings may have superior aerodynamic performance has led to renewed interest in this design. In this report, laminated beam theory, together with aerodynamic strip theory, is used to predict the static aero-

DD FORM 1473 EDITION OF 1 NOV 65 IS OBSOLETE
1 JAN 73

elastic divergence characteristics of swept wings. From the results of this theory, it is predicted that, because of elastic coupling between bending and torsional deformation of the wing box, laminated composites may be used to preclude wing divergence for a large range of wing forward sweep angles. Formulas are developed to illustrate the important parameters governing composite wing divergence. Two examples are presented to illustrate the use of these formulas. These examples show that composite forward swept wings have the potential to be feasible, efficient designs.

FOREWORD

48 12 11 002

TABLE OF CONTENTS

LIST OF ILLUSTRATIONS

LIST OF TABLES

LIST OF SYMBOLS

a_0 = two-dimensional lift-curve slope.

A_{22} = axial stiffness parameter, Equation (A-32).

$\bar{a}$ = aeroelastic parameter, Equation (28).

B_{22} = elastic coupling parameter, Equation (A-33).

B_{33} = elastic coupling parameter, Equation (A-34).

c = wing chord length, measured perpendicular to the reference axis.

$\bar{d}$ = aeroelastic parameter, Equation (29).

e = distance between wing quarter-chord and reference axis, positive aft.

G_{12} = shear modulus of lamina with respect to principal axes.

EI_0 = bending stiffness parameter, Equation (A-28).

f = $1-n(1 - \lambda)$.

E_1, E_2 = lamina moduli of elasticity with respect to principal axes.

g = composite torsional coupling parameter, K/GJ.

GJ_0 = torsional stiffness parameter, Equation (A-29).

$h(y)$ = bending deflection of the reference axis of the wing, positive upward.

k = nondimensional bending coupling parameter, K/EI.

K_0 = bending-torsion coupling parameter, Equation (A-31).

ℓ = wing semi-span dimension, measured along the reference axis.

M_x = bending moment resultant, Equation (B-14).

$p(y)$ = distributed load along reference axis, positive upward.

q = dynamic pressure, $\frac{1}{2}\rho V^2$.

$t(y)$ = distributed torque per unit length, positive nose-up.

T = torque resultant, Equation (B-16).

$v_0(y)$ = axial deformation along reference axis.

V_z = shear force resultant, Equation (B-15).

y = distance along reference axis.

z = distance from beam middle surface, positive upward.

$\alpha(y)$ = torsional deformation of wing sections about the reference axis, positive nose-up.

α_e = $\alpha - \Gamma \tan \Lambda$

Γ = dh/dy

η = y/ℓ

θ = fiber angle with respect to a rearward normal from the reference axis, Figure 2.

λ = taper ratio = c_{tip}/c_{root}.

μ_{12}, μ_{21} = Poisson's ratios.

Λ = sweep angle of the reference axis, positive for sweepback.

SECTION I

INTRODUCTION

The expanding utilization of laminated composite materials in air-
craft structural components has led engineers to seek new ways to utilize
fully these light-weight materials. One aspect of this search has been
the study of aeroelastic tailoring of composite materials. Aeroelastic
tailoring of a lifting surface involves the synthesis of a composite ma-
terial structure whose special directional properties enhance the aero-
elastic performance of the airfoil. Primary attention has been focused
upon improving conventional aircraft designs such as sweptback wing con-
figurations. The purpose of this report is to illustrate the potential
benefits to be gained by applying the aeroelastic tailoring concept to a
nonconventional design, an aircraft with a forward swept wing.

A report by Diederich and Budiansky [1] discusses the aeroelastic
divergence of metallic swept wings. Their report shows convincingly that,
from a static aeroelastic stability point of view, sweptback metallic wings
are far superior to sweptforward metallic wings. As a result of their
study, the forward swept metallic wing has not been a serious design con-
cept for some time.

Although the metallic forward swept wing is inferior, from a structural
stiffness standpoint, the forward swept wing possesses some aerodynamic
advantages over the sweptback wing. Knight and Noyes [2] noted in 1931
that wings with 20° of forward sweep experience stall at higher angles of
attack than similar 20° sweptback wings. Thus, sweptforward wings may
develop higher lift coefficients than similar sweptback wings. In addition,
Jones [3] notes that sweepback may produce a pronounced rolling or pitching

1

instability because of the premature tip stall of these wings. Conversely, at high angles of attack, forward swept wings begin to stall first at the wing root and are not subject to this phenomenon. On the other hand, the inherent lack of directional stability of a forward swept flying wing makes it necessary to provide a generous vertical stabilizer and rudder. Little has been published concerning the stability and control characteristics of forward swept wing-fuselage configurations.

The first aircraft to employ a forward swept wing was the Junkers Ju 287 jet bomber [4] developed in Germany during World War II. This test aircraft flew on 16 occasions in 1944, developing speeds of over 650 km/hr (404 mph). The wing on the Ju 287 was swept forward nearly 25°, primarily to provide good low speed flight characteristics. Limited flight tests, brought to a halt by advancing Soviet armies, did not disclose any severe aeroelastic or directional stability problems. The interested reader will find the information in Reference 4 a fascinating account of a little known chapter in aircraft history.

A modern-day example of an airplane with a forward swept wing is provided by the German Hansa twin-jet executive transport [5]. This aircraft is the only forward swept wing aircraft other than the Ju 287 that has actually flown. Developed by Messerschmitt-Bölkow-Blohm, the prototype HFB 320 Hansa first flew in 1964. The metallic wing on the HFB 320 exhibits an aspect ratio of 6, a taper ratio of 1:3, and employs 15° of forward sweep at the quarter-chord line to avoid the necessity of taking the main spar of the wing through the passenger cabin. The aircraft has a maximum cruise speed of 825 km/hr (513 mph) at 25,000 ft. A stretched version of the HFB 320, designated as the HFB 330 Hansa has also been developed.

2

Renewed interest in forward swept wing technology is due to N. J. Krone, Jr. [6]. Reference 6 illustrates the feasibility of the forward swept wing concept when laminated composite materials, rather than metals, are used in the wing structure. Krone's conclusion, arrived at through a comprehensive set of numerical examples, is that the use of laminated composite materials in the wing structure offers the design flexibility to overcome the weight disadvantages encountered in conventional metallic, forward swept wing design. Thus, proper aeroelastic tailoring appears to lessen the severity of the aeroelastic divergence problem of forward swept wings.

The results in Reference 6 leave unsettled several questions about the basic mechanism by which static aeroelastic stability improvement is achieved through the use of laminated composites. The present report provides a study of the static aeroelastic divergence characteristics of wings whose structure is constructed solely of laminated, fibrous composite materials. This study uses a mathematical idealization of the wing divergence problem similar to that used in Reference 1, but incorporates laminated beam theory into the analysis. Attention is focused upon the additional coupling between bending and torsional deformations of a wing, introduced by the laminated composite construction, and its influence on swept wing divergence.

The mathematical model used throughout the study employs a strip theory representation of the aerodynamic loads that arise from wing bending and torsional deformation of high aspect ratio wings. This representation, together with laminated beam theory, allows the solution of the wing divergence problem in analytical form. Such a solution is useful, since the effect of geometrical, structural and aeroelastic parameters can be seen readily.

3

SECTION II

AEROELASTIC MODEL IDEALIZATION

Some insight into the influence of laminated composite materials upon swept wing design can be found through a mathematical analysis of an idealized model of a slender, high-aspect-ratio wing, such as that shown in Figure 1. This section describes the assumptions used to model both the structural deformation behavior of the wing and the aerodynamic loads due to this deformation. This idealized model will be used to develop closed-form solutions for aeroelastic divergence of swept, composite wings.
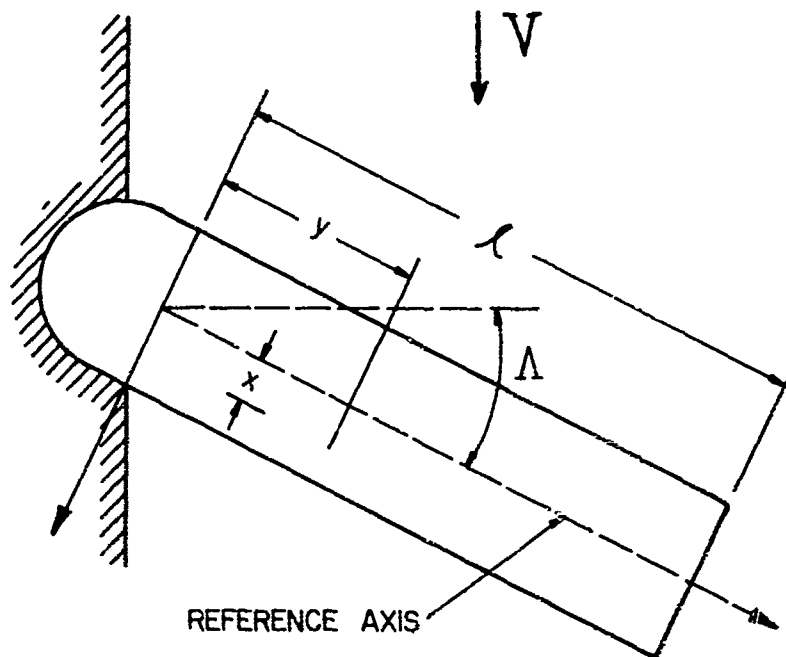
Figure 1 - Geometry and sign convention used for the constant chord swept wing analysis.

1. WING STRUCTURAL DEFORMATION MODEL

The wing shown in Figure 1 is assumed to derive all of its bending and torsional stiffness from thin, laminated composite, cover-sheets that form the upper and lower surfaces of the wing. It is assumed that the resulting box-beam wing structure is such that its deformation may be represented by a bending deflection $h(y)$, positive upward, along a straight reference axis (the y-axis in Figure 1) and a rotation $\alpha(y)$, positive nose-up, about this axis. In addition, it is further assumed that wing chord-wise sections, perpendicular to the beam's reference axis, are rigid so that wing deformation is a function only of the spanwise coordinate, y. The enforcement of this type deformation is essential to the work that follows. A similar structural model is used by Housner and Stein [7] to study the flutter of sweptback laminated composite wings.

Using the box-beam model, equivalent bending and torsional stiffnesses of the wing, EI and GJ, respectively, may be computed employing the classical Euler-Bernoulli assumptions. As is suggested in Reference 7, the derivation of the equivalent EI and GJ for the structure is best accomplished through strain energy methods. The Euler-Bernoulli displacement behavior constrains the individual laminae in the upper and lower laminated cover sheets to act as a unit and supplies the strain-displacement relations for the wing structure. The definition of the stress-strain relations of each of the laminae furnishes the additional information necessary to formulate the strain energy expression for the box-beam.

Attention will now turn to a summary of the development of the expressions for EI and GJ. Since terms that involve the individual lamina stress-strain properties appear in the expressions for EI and GJ, the

5

development of the stress-strain relations for the lamina will be reviewed.
A full discussion of the development of the equilibrium equations that
govern the laminated beam is contained in Appendices A and B.
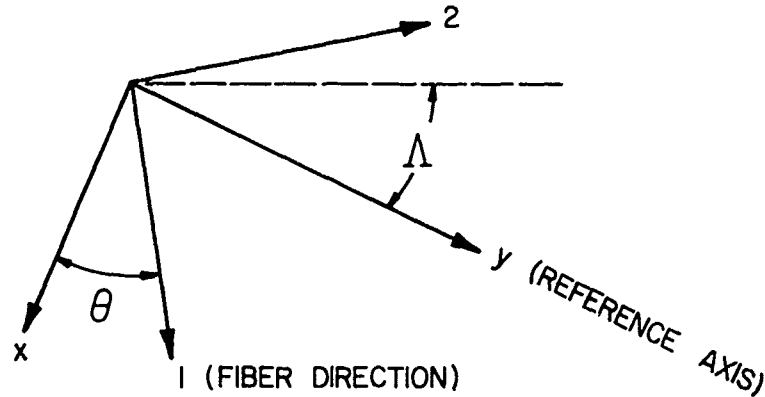
Figure 2 - Composite material lamina principal
axes, 1 and 2, with respect to the
wing reference axes, x and y.

Each lamina of the box-beam is itself orthotropic with respect to a
set of principal axes, one axis being oriented in the direction of the
lamina fibers, while the other axis is perpendicular to these fibers. These
principal axes, denoted as axis 1 and axis 2 and shown in Figure 2, lie in
a plane parallel to the x-y reference plane of the wing, but are oriented
at an angle θ with respect to the x-y system. The angle θ is measured
positive in the counterclockwise direction from the x-axis shown in Figure 2.

As shown in Reference 8, the relationship between inplane stresses
and strains may be written, for a single orthotropic lamina, as

$$
\left\{
\begin{array}{c}
\sigma_{xx} \\
\sigma_{yy} \\
\tau_{xy}
\end{array}
\right\} =
\left[
\begin{array}{ccc}
\bar{Q}_{11} & \bar{Q}_{12} & \bar{Q}_{16} \\
\bar{Q}_{12} & \bar{Q}_{22} & \bar{Q}_{26} \\
\bar{Q}_{16} & \bar{Q}_{26} & \bar{Q}_{66}
\end{array}
\right]
\left\{
\begin{array}{c}
\epsilon_{xx} \\
\epsilon_{yy} \\
\gamma_{xy}
\end{array}
\right\}
\tag{1}
$$

The terms $\overline{Q}_{ij}$ are functions of θ, the fiber angle, and the orthotropic engineering constants Q_{ij} given by the following expressions.

$$Q_{11} = E_1/(1 - \mu_{12}\mu_{21}) \tag{2a}$$

$$Q_{12} = \mu_{12} E_2/(1 - \mu_{12}\mu_{21}) \tag{2b}$$

$$= \mu_{21} E_1/(1 - \mu_{21}\mu_{12})$$

$$Q_{22} = E_2/(1 - \mu_{12}\mu_{21}) \tag{2c}$$

$$Q_{66} = G_{12} \tag{2d}$$

The terms $\overline{Q}_{ij}$ are defined in a convenient manner by first defining a set of parameters U_1 that are functions of Q_{ij} [8].

$$U_1 = [3Q_{11} + 3Q_{22} + 2Q_{12} + 4Q_{66}]/8 \tag{3a}$$

$$U_2 = [Q_{11} - Q_{22}]/2 \tag{3b}$$

$$U_3 = [Q_{11} + Q_{22} - 4Q_{66}]/8 \tag{3c}$$

$$U_4 = [Q_{11} + Q_{22} + 6Q_{12} - 4Q_{66}]/8 \tag{3d}$$

$$U_5 = [Q_{11} + Q_{22} - 2Q_{12} + 4Q_{66}]/8 \tag{3e}$$

In terms of these new parameters U_i and the angle θ, the $\overline{Q}_{ij}$ terms become

$$\overline{Q}_{11} = U_1 + U_2\cos2\theta + U_3\cos4\theta \tag{4a}$$

$$\overline{Q}_{12} = U_4 - U_3\cos4\theta \tag{4b}$$

$$\overline{Q}_{22} = U_1 - U_2\cos2\theta + U_3\cos4\theta \tag{4c}$$

$$\overline{Q}_{16} = \frac{1}{2} U_2\sin2\theta + U_3\sin4\theta \tag{4d}$$

$$\overline{Q}_{26} = \frac{1}{2} U_2\sin2\theta - U_3\sin4\theta \tag{4e}$$

$$\overline{Q}_{66} = U_5 - U_3\cos4\theta \tag{4f}$$

7

Since the individual laminae are constrained to act as a unit, in a manner prescribed by the Euler-Bernoulli deformation assumptions, a strain energy functional can be constructed by summing the individual strain energies of each lamina. The reference surface for this strain energy expression is the middle surface of the wing box. The total strain energy, denoted as U, is written as follows (note that $(\ )' = d(\ )/dy$):

$$U = \int_0^\ell \left\{ \frac{1}{2} EI_0(h'')^2 - K_0(h''\alpha') + \frac{1}{2} A_{22}(v_0')^2 \right.$$
$$\left. + B_{33}(v_0'\alpha') - B_{22}(h''v_0') + \frac{1}{2} GJ_0(\alpha')^2 \right\} dy \qquad (5)$$

The terms multiplying the deflection derivatives in Equation (5) are defined in Appendix A. These terms are linear functions of the wing chord and also involve the $\overline{Q}_{ij}$ parameters of the individual laminae.

From Equation (5) it is seen that the bending deformation $h(y)$ is elastically coupled both to the torsional deformation $\alpha(y)$ and to the extensional deformation of the middle surface, $v_0(y)$. The extensional deformation $v_0(y)$ will be zero if the middle surface is also the neutral surface for bending, a situation that occurs if the upper and lower laminated cover sheets are oriented symmetrically with respect to the middle surface.

The Principle of Virtual Work is used to derive the differential equations governing the static equilibrium of the laminated beam under the action of the upward distributed load $p(y)$ and a distributed torque $t(y)$. These equations, derived in Appendix B, are

$$[EIh'' - K\alpha']'' = p(y) \qquad (6)$$
$$[-Kh'' + GJ\alpha']' = -t(y) \qquad (7)$$

Note that in Equations (6) and (7) $(\ )' = d(\ )/dy$. The terms EI, GJ and K

8

are related to the parameters in Equation (5) by the expressions

$$EI = EI_0 - (B_{22})^2/A_{22} \tag{8a}$$

$$GJ = GJ_0 - (B_{33})^2/A_{22} \tag{8b}$$

$$K = K_0 - B_{22}B_{33}/A_{22} \tag{8c}$$

Equations (8a,b,c) are the result of the elimination of the v_0 degree of freedom from the problem, an operation described in detail in Appendix B.

Equations (6) and (7) are coupled together by the parameter K, a term that, in general, is nonzero for a laminated material. The K parameter provides an elastic coupling between bending and torsion not found in metallic beam analysis. Since K depends upon both the stacking sequence used in constructing the laminate and the lamina fiber orientation angles, an opportunity to tailor the wing structure to provide advantageous bending-torsion coupling is presented.

Boundary conditions for the cantilevered wing consist of the displacement and slope conditions at the wing root,

$$\alpha(0) = h(0) = \frac{dh}{dy}(0) = 0 \tag{9a,b,c}$$

and the bending moment, shear and torque conditions at the tip, written as:

$$M(\ell) = EIh'' - K\alpha' = 0 \tag{10a}$$

$$V(\ell) = [EIh'' - K\alpha']' = 0 \tag{10b}$$

$$T(\ell) = GJ\alpha' - Kh'' = 0 \tag{10c}$$

2. IDEALIZATION OF WING AERODYNAMIC LOADS

Aerodynamic strip theory provides a meaningful and somewhat accurate way of describing, in mathematical terms, the air loads acting upon a slender wing as the result of structural deformation. A complete discussion

9

of this aerodynamic formulation is given in Reference 9.

The aerodynamic forces and moments acting upon wing segments that are perpendicular to the reference axis (the y-axis) of the wing may be computed, provided an effective wing root and tip are assumed, an assumption that may involve some error. However, the strip theory approach produces simple equations that have been shown to give satisfactory results for large aspect ratio metallic wings.
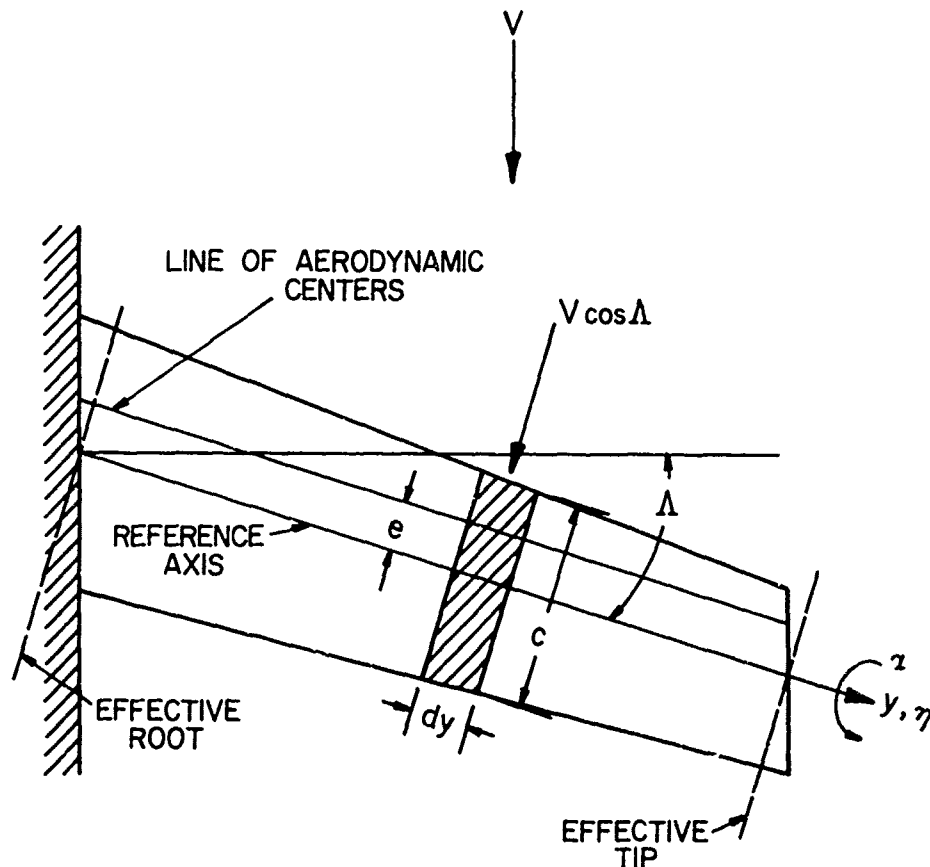
Figure 3 - Slender swept wing geometry used to describe aerodynamic loads, showing chordwise segments perpendicular to the swept reference axis.

To formulate the divergence problem, the only aerodynamic loads to be considered are those caused by deformation $h(y)$ and $\alpha(y)$. Figure 3 defines the geometrical parameters used to define these aerodynamic loads. In terms of the upward deflection of the reference axis, $h(y)$, and the torsional rotation, $\alpha(y)$, of the wing chordwise sections, about this axis, the lift force per unit length, positive upward, is

$$p(y) = qca_0\cos^2\Lambda(\alpha - \frac{dh}{dy}\tan\Lambda) \tag{11}$$

The torque per unit length due to structural deformation is expressed as

$$t(y) = qcea_0\cos^2\Lambda(\alpha - \frac{dh}{dy}\tan\Lambda) \tag{12}$$

The term a_0 appearing in Equations (11) and (12) is the two-dimensional lift curve slope of the wing sections.

The lift curve slope can be empirically corrected to reflect the effects of finite span, wing sweep and compressibility. The present report makes no modification of the 2-D lift curve slope to account for compressibility. However, the 2-D lift curve slope is empirically corrected to take into account aspect ratio, AR, and sweep angle Λ by applying the correction

$$a_0 = a_0(\Lambda=0)\left[\frac{AR}{AR + 4\cos\Lambda}\right] \tag{13}$$

Equation (13) is adapted from that used in Reference 1.

Equations (11) and (12) are inserted into Equations (6) and (7), respectively, to provide the differential equations governing the aeroelastic divergence of composite swept wings. The solution to these equations for several cases is discussed in the ensuing sections.

3. DIVERGENCE OF A UNIFORM CHORD WING WITH BENDING FLEXIBILITY ONLY

The simplest wing divergence case to consider is one in which the wing

11

has constant geometrical and stiffness properties along its span and has no torsional flexibility. For this case, the governing equation of equilibrium becomes

$$EIh^{iv} + qca_0(\frac{dh}{dy}) \sin\Lambda\cos\Lambda = 0 \qquad (14)$$

Equation (14) can be transformed into the following nondimensional form:

$$\frac{d^3\Gamma}{d\xi^3} - b\Gamma = 0 \qquad (15)$$

by defining the new variables

$$\Gamma = \frac{dh}{dy} \qquad \xi = 1 - y/_\ell \qquad b = \frac{qca_0\ell^3\sin\Lambda\cos\Lambda}{EI}$$

Boundary conditions for this cantilever wing problem, in terms of the variable ξ, are:

$$\Gamma(1) = 0, \quad \frac{d\Gamma(0)}{d\xi} = 0, \quad \frac{d^2\Gamma(0)}{d\xi^2} = 0 \qquad (16a,b,c)$$

This problem is an eigenvalue problem and is discussed at length in Reference 10 (pp. 311 - 317). The solution to this problem yields a critical value of dynamic pressure, q, at divergence, denoted as q_D, given by the following expression:

$$q_D = \frac{6.33 \ EI}{a_0 c\ell^3 |\sin\Lambda|\cos\Lambda} \qquad (17)$$

Equation (17) is valid only if Λ, the sweep angle, is less than zero; this value of Λ occurs when the wing is sweptforward. A sweptback wing ($\Lambda>0$) will not diver.. .nder the present assumptions.

With no torsional deformation permitted, the dynamic pressure at divergence is maximized by maximizing the parameter EI. The maximum value of

the parameter EI is attained, in the case of a fibrous composite, by aligning the fibers parallel to the swept reference axis. This result is not surprising and, indeed, is somewhat discouraging, because the solution to designing such a structure lies in adding more composite material as the wing is sweptforward. This strategy is identical to that followed for conventional metallic designs.

4. DIVERGENCE OF A SWEPT WING WITH UNIFORM GEOMETRICAL AND STRUCTURAL PROPERTIES - BENDING AND TORSION INCLUDED

a. Equilibrium Equations

The coupled differential equations that govern aeroelastic divergence of a constant chord, laminated composite, swept wing with both bending and torsional flexibility are written as:

$$EIh^{iv} - K\alpha''' = (qca_0\cos^2\Lambda)(\alpha - h'\tan\Lambda) \tag{18}$$

and

$$GJ\alpha'' - Kh''' = -(qca_0e\cos^2\Lambda)(\alpha - h'\tan\Lambda) \tag{19}$$

where $(\ )' = d(\ )/dy$.

To nondimensionalize the above equations and thus facilitate the solution, three new variables are defined:

$$\eta = y/_\ell, \quad w = h/_\ell, \quad \Gamma = \frac{dh}{dy} = \frac{dw}{d\eta} \tag{20a,b,c}$$

These new variables permit Equations (18) and (19) to be expressed as:

$$\Gamma''' - k\alpha''' = a(\alpha - \Gamma\tan\Lambda) \tag{21}$$

$$\alpha'' - g\Gamma'' = -b(\alpha - \Gamma\tan\Lambda) \tag{22}$$

where now $(\ )' = d(\ )/d\eta$. Parameters in the above expressions are defined as follows:

13

$$a = qc\ell^3 a_0 \cos^2 \Lambda / EI \qquad (23a)$$

$$b = qce\ell^2 a_0 \cos^2 \Lambda / GJ \qquad (23b)$$

$$k = K/EI \qquad (23c)$$

$$g = K/GJ \qquad (23d)$$

The boundary conditions for these equations are written as follows:

$$\Gamma(0) = 0 \qquad (24a)$$

$$\alpha(0) = 0 \qquad (24b)$$

$$\Gamma'(1) - k\alpha'(1) = 0 \qquad (24c)$$

$$\alpha'(1) - g\Gamma'(1) = 0 \qquad (24d)$$

$$\Gamma''(1) - k\alpha''(1) = 0 \qquad (24e)$$

Equations (21) and (22) can be combined into a single equation by defining a new variable, α_e, given by the relationship

$$\alpha_e = \alpha - \Gamma \tan\Lambda \qquad (25)$$

The variable α_e represents the angle of attack of a chordwise section induced by the torsional and bending deformations of the wing. The steps necessary to accomplish the combination of these two equations into a single equation are outlined in Appendix C. The resulting equation is a third order differential equation with constant coefficients,

$$\alpha_e''' + \left[\frac{b(1-k \tan\Lambda)}{(1 - kg)}\right] \alpha_e' - \left[\frac{a(g - \tan\Lambda)}{(1 - kg)}\right] \alpha_e = 0 \qquad (26)$$

Equation (26) has boundary conditions given by

$$\alpha_e(0) = 0, \quad \alpha_e'(1) = 0 \qquad (27a,b)$$

and

$$\alpha_e''(1) + \left[\frac{b(1 - k \tan\Lambda)}{1 - kg}\right] \alpha_e(1) = 0 \qquad (27c)$$

If the parameters k and g are zero, Equation (26) and its associated boundary conditions reduce to those developed in Reference 1 for the study of

divergence of a metallic wing.

Two aeroelastic parameters appear in Equation (26). These parameters are defined, for ease of notation, as

$$\bar{a} = \left[\frac{1-k\ \tan\Lambda}{1-kg}\right]\left[\frac{qce\ell^2 a_0\cos^2\Lambda}{GJ}\right] \qquad (28)$$

$$\bar{d} = \left[\frac{\tan\Lambda - g}{1-kg}\right]\left[\frac{qc\ell^3 a_0\cos^2\Lambda}{EI}\right] \qquad (29)$$

b. Solution to the Divergence Equations

The solution to the eigenvalue problem defined by Equation (26) and its boundary conditions, Equations (27a,b,c), follows that given in Reference 1. This solution is summarized in Appendix C of the present report.

Figure 4 displays the interdependence of the critical values of $\bar{a}$ and $\bar{d}$ found for this problem. The region above the solid curve shown in Figure 4 represents a region in which combinations of values of $\bar{a}$ and $\bar{d}$ result in a divergence condition for the swept wing. Values of $\bar{a}$ and $\bar{d}$ below the solid curve correspond to those values of the aeroelastic parameters that are associated with a stable wing. Thus, the solid curve corresponds to a stability boundary for the constant chord wing.

As discussed in Reference 1, an approximation to the curve shown in Figure 4 provides an accurate approximate relation between $\bar{a}_D$ and $\bar{d}_D$, the values of $\bar{a}$ and $\bar{d}$ at divergence. This approximation is developed by first recognizing that $\bar{a}$ is equal to zero if the wing is rigid in torsion. This condition corresponds to bending divergence of a swept wing, discussed in Section II, part 3. In this case,

$$\bar{d}_D = \frac{-19}{3} = -6.333 \qquad (30)$$

If the wing is rigid in bending, but has torsional flexibility, then $\bar{d} = 0$

15
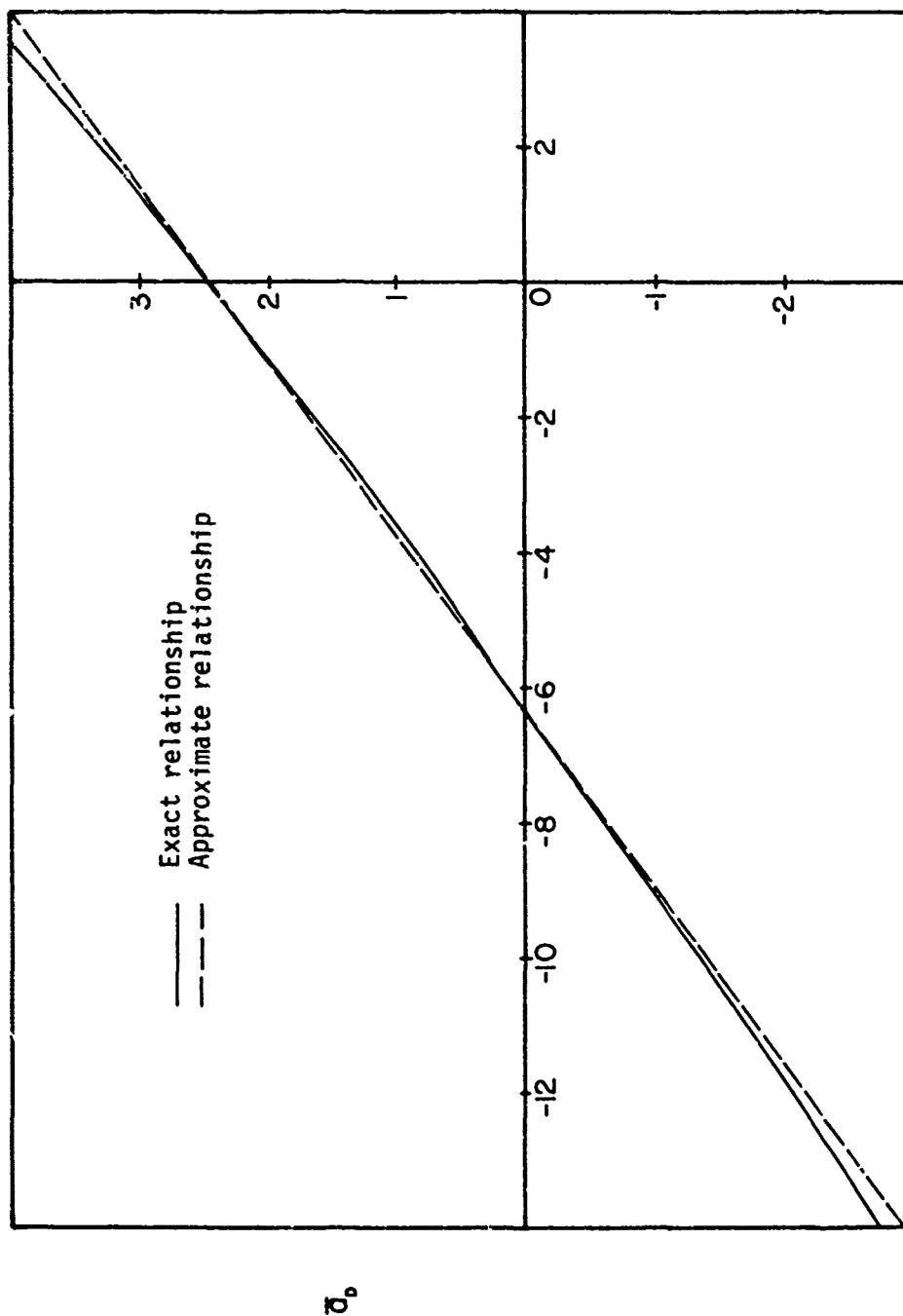
Figure 4 - The relationship between the wing divergence parameters $\underline{a}$ and $\underline{d}$ for a constant chord, uniform property wing; the stability boundary relating a_D to $\bar{d}_D$ is indicated by the solid line. (Adapted from NACA TN No. 1680).

and the exact solution to the divergence problem results in a value of $\bar{a}_D$ given by

$$\bar{a}_D = \left(\pi/_2\right)^2 \qquad (31)$$

If a linear algebraic relationship between $\bar{a}_D$ and $\bar{d}_D$ is assumed, taking into account the results in Equations (30) and (31), an approximate relationship between $\bar{a}_D$ and $\bar{d}_D$ can be developed. This relationship is given by the equation

$$\bar{a}_D = \left(\frac{\pi}{2}\right)^2 + \left(\frac{3\pi^2}{76}\right)\bar{d}_D \qquad (32)$$

The approximate relationship given by Equation (32) is shown as a dashed line in Figure 4. For the range of values shown in this figure, the agreement between the exact solution and the approximate solution is excellent.

Combining Equations (28) and (29) with Equation (32), the dynamic pressure at divergence is found to be

$$q_D = \left[\frac{2.47\ (1 - kg)}{c\ell^2 a_0 \cos^2\Lambda}\right]\left[\frac{EI}{\frac{1 - k\ \tan\Lambda}{(\frac{\ell}{e})\ (\frac{GJ}{EI})} - 0.39(\tan\Lambda - g)}\right] \qquad (33)$$

Equation (33) provides useful information about the divergence behavior of the swept wing. First of all, if q_D is a negative number, no real divergence speed occurs, since the airspeed V must be an imaginary number if q_D is to be less than zero. Therefore, combinations of parameters that result in negative values of q_D are desirable. From strain energy considerations, the factor $(1 - kg)$ in Equation (33) will always be a positive number. Thus, the denominator, containing terms dependent upon Λ and the geometric and structural characteristics of the wing, controls the sign of q_D.

17

The divergence dynamic pressure q_D changes sign at infinity. The parameter q_D becomes infinite when the following relationship is satisfied:

$$\tan \Lambda_{cr} = \frac{g + 2.56 \left(\frac{e}{\ell}\right)\left(\frac{EI}{GJ}\right)}{1 + 2.56 \left(\frac{e}{\ell}\right) g} \tag{34}$$

Values of tan Λ larger than that given in Equation (34) result in finite negative values of q_D that, in turn, yield imaginary divergence velocities. The value of Λ determined in Equation (34) is denoted as Λ_{cr} because it represents that value of the sweep angle above which swept wing divergence is theoretically impossible.

To interpret and to compare the information provided by Equation (34), it is noted that a conventional metallic wing has the parameter g equal to zero. Thus, Λ_{cr} is a constant for the metallic wing. For a laminated composite wing, Λ_{cr} will be a function of the laminate characteristics. Furthermore, for a metallic wing operating at subsonic speeds, Λ_{cr} will be greater than zero for the usual case in which the parameter e is greater than zero. This means that the metallic wing must be swept back to preclude divergence. On the other hand, with a composite material wing for which the parameter g is less than zero, the possibility exists that Λ_{cr} is less than zero. In this case, sweep angles exist, in the forward swept range, for which divergence will not occur at any flight speed.

c. Example Cases

An example of the use of Equation (34) to study divergence is provided by two related wing configurations. In the first case, all of the laminate fibers of the cover sheets are oriented along a common direction, denoted as the angle θ. In the second case, 10% of the fibers are fixed at an

18

angle $\theta = 0°$, 25% of the fibers are oriented symmetrically at $\theta = \pm 45°$ (12.5% are + 45°, 12.5% are -45°), while the remaining 65% of the laminate has fibers oriented at an angle θ. Geometric and lamina material data for the wing are as follows:

Wing and Lamina Properties

Wing Aspect Ratio, AR = 6   Offset between aerodynamic center and reference axis, e = 0.10c

Lamina Material: Boron-epoxy

$E_1 = 32.5 \times 10^6$ psi. (tension)

$E_2 = 3.2 \times 10^6$ psi. (tension)

$G_{12} = 1.05 \times 10^6$ psi. $\mu_{12} = 0.36$

The ratio of box-beam depth to cover-sheet thickness is 20:1.

Figure 5 shows the relationship between the parameter g=K/GJ and θ for each case. For Case 1, in which 100% of the fibers can be tailored, the absolute value of g has a maximum value of about 1.20. Also to be noted is that g is an asymmetrical function (about $\theta = 90°$) of θ. In Case 2, where only 65% of the fibers are available for design orientation, a reduction in the percentage of fibers that can be used for tailoring is seen to result in a decrease in the maximum absolute value of g to near $|g| = 0.50$. In addition, the position of the min-max values of g in the latter case lies farther away from the $\theta = 90°$ position than that found for Case 1. It should be noted that both EI and GJ are symmetrical functions of θ (about $\theta = 90°$).

Using Equation (34), the relationship between Λ_{cr} and θ for the two previously discussed cases can be determined. These results are shown in Figure 6. In Case 1, proper orientation of the laminate fibers can preclude

19
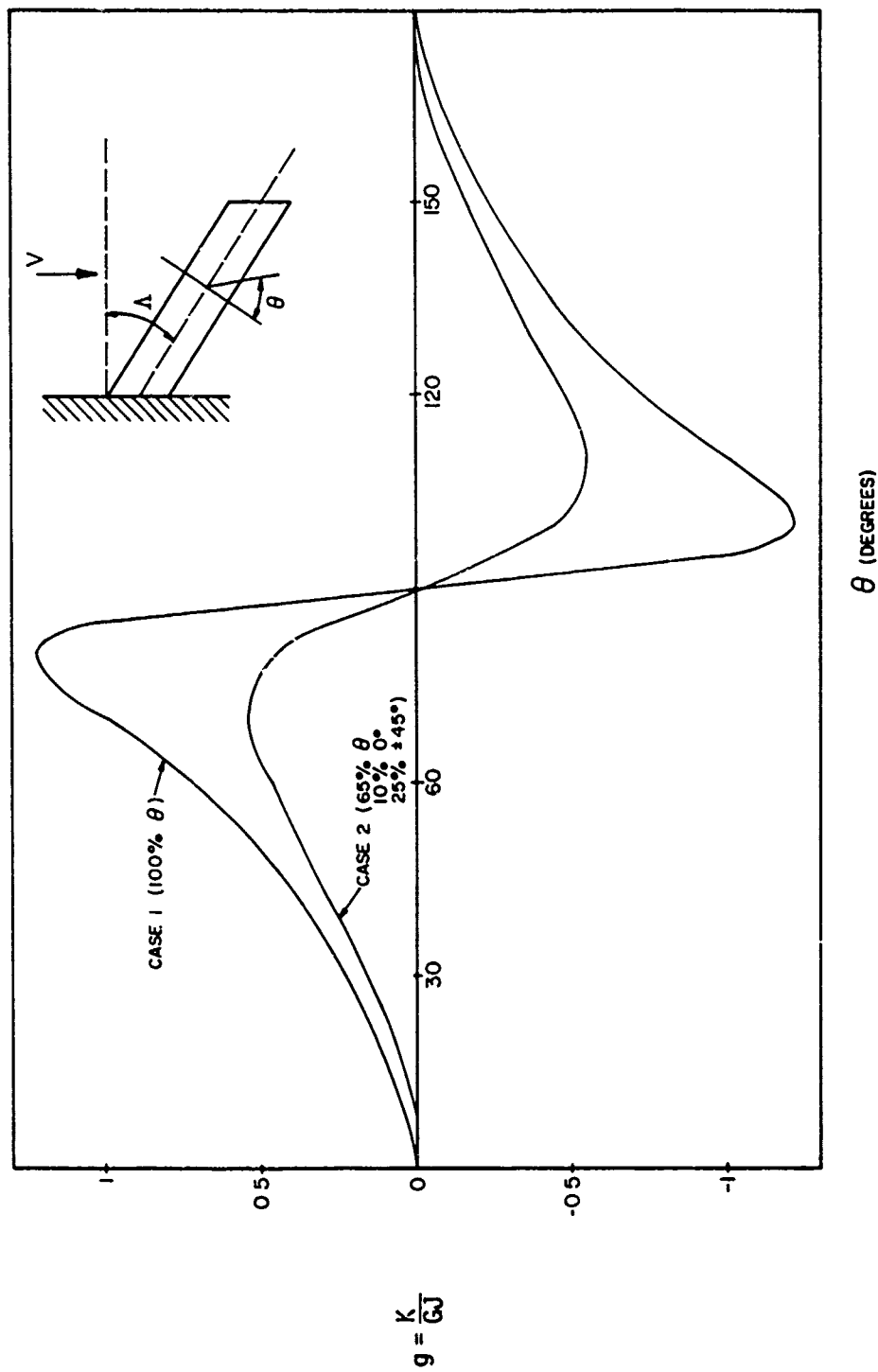
Figure 5 - The relationship between the elastic coupling parameter g=K/GJ and the fiber angle θ for two example laminates.

20

wing divergence until a forward sweep angle of nearly 49°. This occurs if laminate fibers are oriented at an angle about 12° ahead of the swept reference axis ($\theta = 102°$). For Case 2, in which fewer fibers are used in the tailoring process, the results are less dramatic, but still impressive. When θ is about 110° (20° forward of the reference axis) the wing may still be swept forward nearly 28° before a real divergence speed is encountered.

Figure 7 shows the behavior of the divergence speed V_D of the uniform property wing in Case 1 as the fiber angle changes. The results are normalized with respect to V_{DO}, the value of V_D that results when the wing is unswept and all the fibers are oriented along $\theta = 0$. Three sweep angles are considered in Figure 7; these angles are $\Lambda = 0°$, $-30°$, $-60°$, corresponding to an unswept wing and two forward swept wings. In the range $0° \leq \theta < 90°$, the divergence speeds of the wing for each of the sweep angles are relatively low. However, as θ is increased beyond 90° and the fibers are rotated forward of the wing reference axis, the divergence speed increases rapidly. In the cases of the unswept wing and the wing with 30° of forward sweep, the divergence speed becomes infinite for fiber angles $\theta = 95°$. There is a range of laminate fiber angles for which divergence is impossible in these latter two sweep cases. The range of angles in which divergence is precluded is seen to decrease with increasing forward sweep. Referring back to Figure 6, it is to be expected that this range or bandwidth approaches zero as the angle of forward sweep approaches 49°. Returning to Figure 7, it is seen that, for $\Lambda = -60°$, a maximum divergence speed is reached when θ is approximately equal to 100°. For this fiber orientation, this particular forward swept wing has the same divergence speed as an unswept wing with all the fibers oriented along the reference
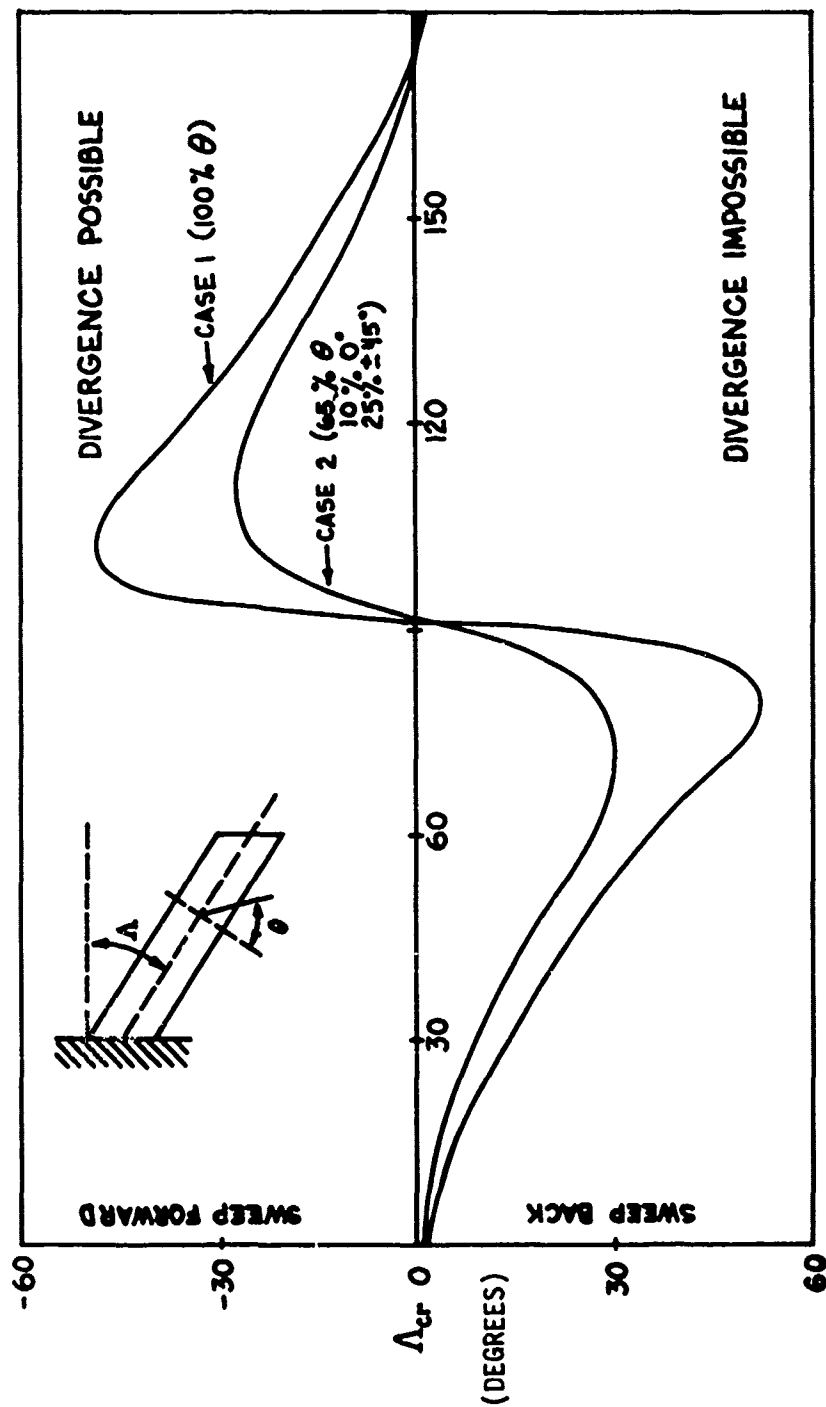
Figure 6 - The relationship between the critical sweep angle, Λ_{cr}, and the fiber orientation angle θ for two example laminates. Finite divergence speeds will exist for sweep angles that lie in the region above the curves. Uniform wing.

22
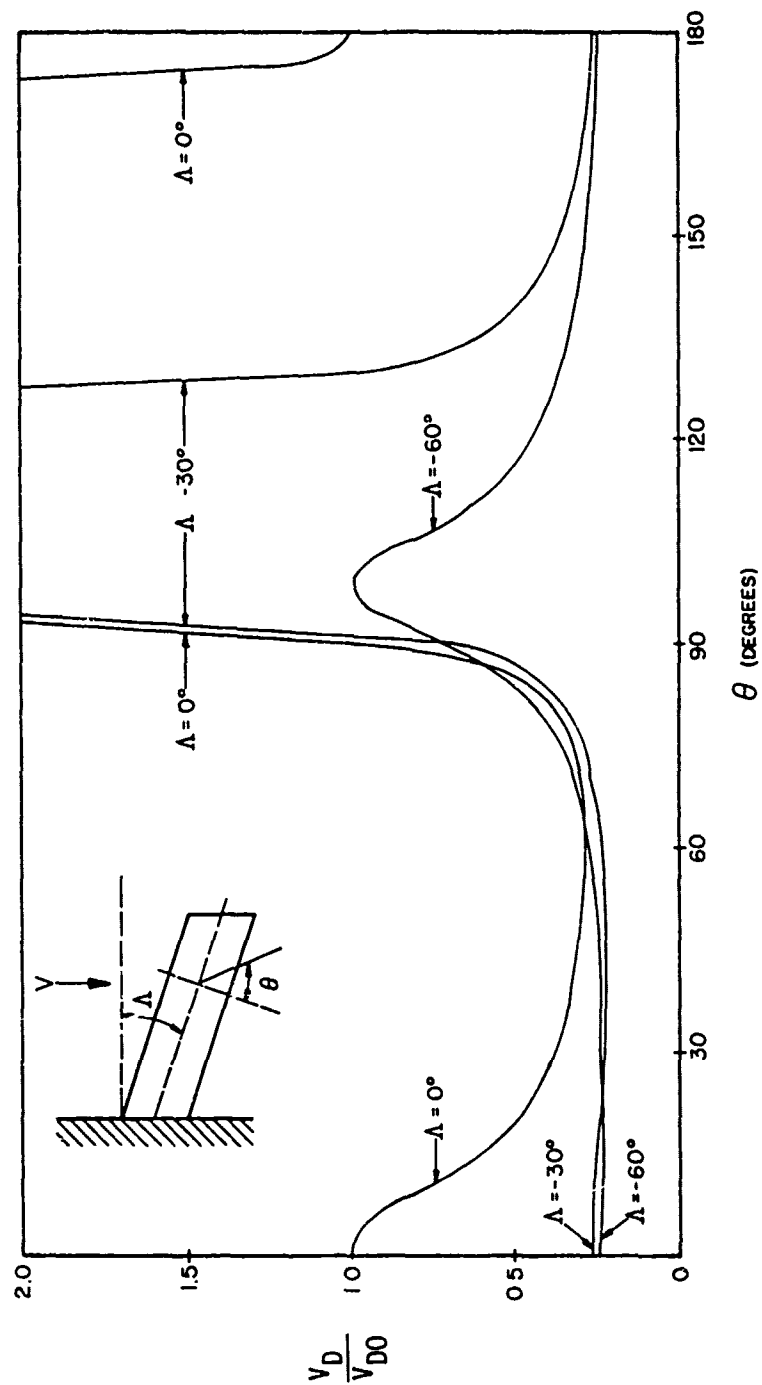
Figure 7 - Normalized divergence speed V_D/V_{D0} versus fiber angle θ for a laminate with all fibers oriented at an angle θ. Uniform wing; three different sweep angles. Wing box depth to top or bottom cover sheet thickness is 20:1.

23

axis ($\theta = 90°$).

An additional, important feature of Figure 7 is that the divergence behavior of the unswept wing is not symmetrical about $\theta = 90°$, even though EI and GJ are symmetrical functions about that position. For a metallic wing at zero sweep, the divergence speed is independent of the bending stiffness, since bending deformation produces no lift. However, in the case of the laminated composite wing, bending deformation, caused by lift, causes torsional deformation that, in turn, leads to changes in lift. This elastic coupling feature is clearly seen in Figure 7.

5. DIVERGENCE OF LINEARLY TAPERED WINGS WITH GEOMETRICALLY SIMILAR CROSS-SECTIONS

Next in order of complexity, after the uniform property wing, is a wing whose properties have a linear variation along the wing span. A solution to Equations (6) and (7) is discussed in Reference 1 for the metallic wing whose wing chord varies linearly along the span while the bending and torsional stiffnesses vary as the fourth power of the chord. Such a case occurs when a wing has geometrically similar cross-sections. For a composite wing, the parameter K also varies as the fourth power of the chord if both geometrically similar cross-sections are used and the chord varies linearly with distance along the span.

With the assumptions of linearly varying chord and geometrically similar cross-sections, expressions for the problem parameters are given by the following:

$$c = fc_{root} = fc_r, \quad e = fe_r, \quad EI = f^4 EI_r, \quad GJ = f^4 GJ_r,$$

$$K = f^4 K_r$$

(35)

24

where $f = 1 - {}_n(1 - \lambda)$

λ = wing taper ratio = c_{tip}/c_{root}

$( )_r$ = parameter value evaluated at the wing root.

Transforming Equation (6) to the independent variable f and then nondimensionalizing, gives the bending equation (note that now $( )' = d( )/df$):

$$f^3[\Gamma''' - k_r\alpha'''] + 8f^2[\Gamma'' - k_r\alpha''] + 12f[\Gamma' - k_r\alpha'] - d_T\Gamma + \frac{d_T\alpha}{\tan\Lambda} = 0$$

(36)

where

$$d_T = \frac{qc_r\ell^3a_0\sin\Lambda\cos\Lambda}{EI_r(1 - \lambda)^3}$$

(37)

Similarly, the torsion equation is found from Equation (7) to be

$$f^2[\alpha'' - g_r\Gamma''] + 4f[\alpha' - g_r\Gamma'] + a_T[\alpha - \Gamma\tan\Lambda] = 0$$

(38)

where

$$a_T = \frac{qc_re_r\ell^2a_0\cos^2\Lambda}{GJ_r(1 - \lambda)^2}$$

(39)

Boundary conditions on displacement are, at f = 1 ($\eta = 0$),

$$\alpha(1) = 0, \quad \Gamma(1) = 0$$

(40a,b)

The boundary conditions at $f = \lambda$ ($\eta = 1$) for bending moment, shear force and torque are

$$M(\lambda) = \Gamma'(\lambda) - k_r\alpha'(\lambda) = 0$$

(40c)

$$V(\lambda) = 4\lambda^3(\Gamma'(\lambda) - k_r\alpha'(\lambda)) + \lambda^4(\Gamma''(\lambda) - k_r\alpha''(\lambda)) = 0$$

(40d)

$$T(\lambda) = \alpha'(\lambda) - g_r\Gamma'(\lambda) = 0$$

(40e)

Appendix C, Section 2, details how Equations (36) and (38) may be

25

combined into a single equation in terms of the variable $\alpha_e = \alpha - \Gamma \tan\Lambda$. This single governing equation reads as follows:

$$f^3\alpha_e''' + 8f^2\alpha_e'' + (12 + \bar{a}_T)f\alpha_e' + (2\bar{a}_T - \bar{d}_T)\alpha_e = 0 \tag{41}$$

where the aeroelastic parameters $\bar{a}_T$ and $\bar{d}_T$ are given by

$$\bar{a}_T = \left[\frac{1 - k_r\tan\Lambda}{1 - k_r g_r}\right]\left[\frac{qe_r c_r \ell^2 a_0 \cos^2\Lambda}{GJ_r(1 - \lambda)^2}\right] \tag{42}$$

$$\bar{d}_T = \left[\frac{\tan\Lambda - g_r}{1 - k_r g_r}\right]\left[\frac{qc_r \ell^3 a_0 \cos^2\Lambda}{EI_r(1 - \lambda)^3}\right] \tag{43}$$

The boundary condition for Equation (41) at $f = 1$ ($n = 0$) is:

$$\alpha_e(1) = 0 \tag{44a}$$

At $f = \lambda$, the conditions that $M(\lambda) = 0$ and $T(\lambda) = 0$ give

$$\alpha_e'(\lambda) = 0 \tag{44b}$$

The requirement that there be zero shear at the wing tip, when combined with Equation (38), evaluated at $f = \lambda$, provides the following equation.

$$\lambda^2\alpha_e''(\lambda) + \bar{a}_T\alpha_e(\lambda) = 0 \tag{44c}$$

Equation (41) is an Euler differential equation that can be reduced to a linear differential equation with constant coefficients by changing the variable f to $f = e^t$. The details of solving Equation (41) subject to the given boundary conditions is presented both in Reference 1 and Reference 9 (pp. 486 - 487). These details are omitted here.

As in the case of the uniform property wing, the solution to the equations governing divergence of a tapered wing gives critical values of $\bar{a}$ and $\bar{d}$ that occur at divergence. These critical values, denoted as $\bar{a}_D$

26

$\overline{d}_D$ are plotted in Figure 8 for several wing taper ratios. An approximate linear relationship again can be developed between q_D and the geometrical, structural and aerodynamic parameters in the problem. This relationship is given by the expression:

$$q_D = \left[\frac{GJ_r}{a_0 c_r \ell^3 \cos^2 \Lambda}\right]\left[\frac{\ell}{e_r}\right]\left[\frac{K_1(1 - k_r g_r)}{1-k_r \tan \Lambda - K_2\left(\frac{GJ_r}{EI_r}\right)\left(\frac{\ell}{e_r}\right)(\tan \Lambda - g_r)}\right] \quad (45)$$

The constants K_1 and K_2 are functions of the taper ratio λ and the eigenvalues found for each taper ratio. These constants are tabulated, for several values of λ, in Table 1.

TABLE 1. - VALUES OF K_1 AND K_2 FOR FOUR VALUES OF TAPER RATIO, $\lambda = c_t / c_r$.

λ	K_1	K_2
0.20	2.83	0.614
0.50	2.73	0.497
1.00	2.47	0.390
1.50	2.22	0.326

The effect of taper upon the divergence of swept composite wings can be seen by considering the example for which all fibers in the laminate are oriented at an angle θ. The effect on Λ_{cr} of the taper ratio is shown in Table 2 on page 29.

27
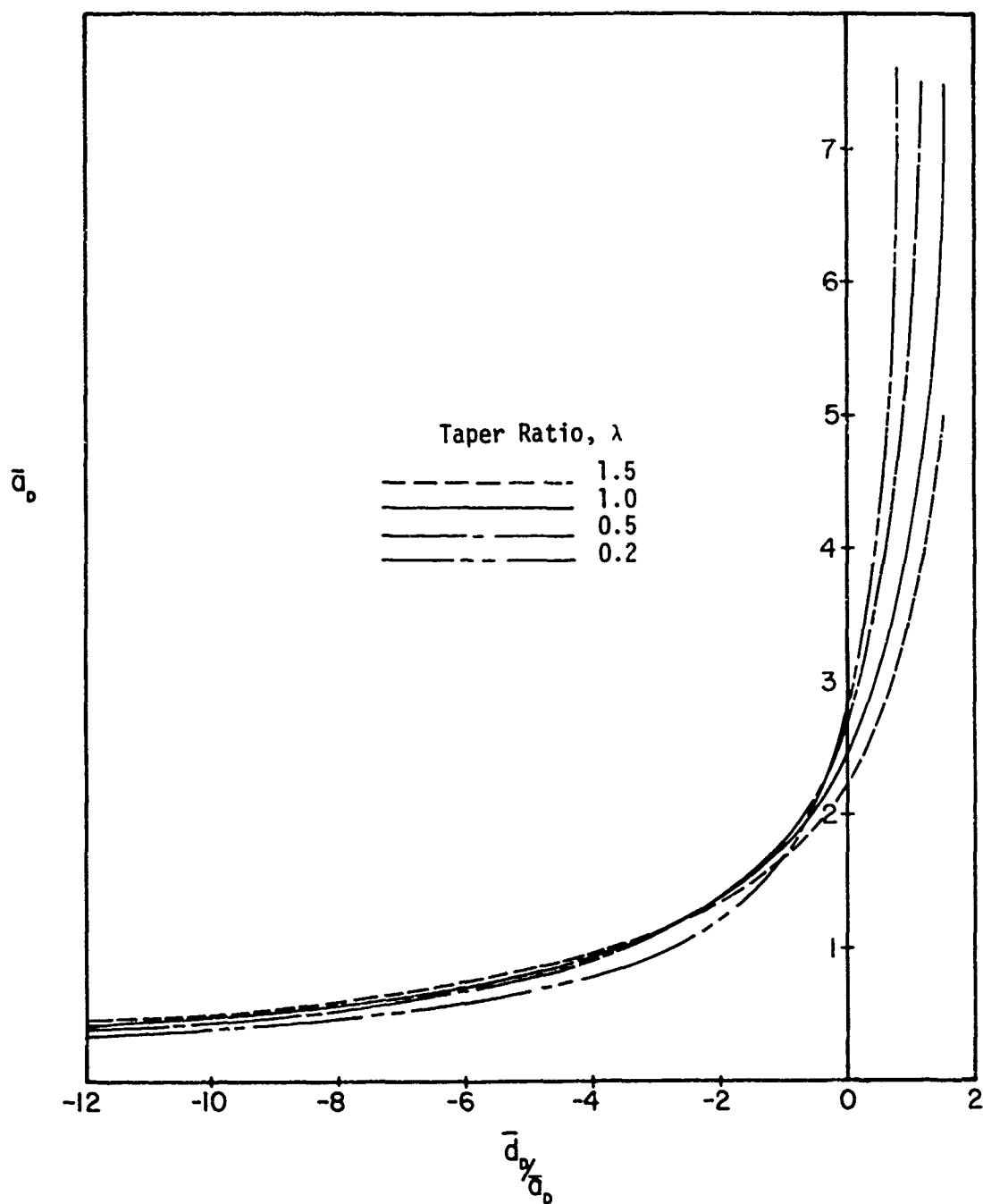
Figure 8 - Swept wing divergence parameters $\bar{a}_D$ versus $\bar{d}_D/\bar{a}_D$ for several wing taper ratios. (Adapted from NACA TN No. 1680).

TABLE 2. - Λ_{cr} VERSUS θ FOR THREE TAPER RATIOS, $\lambda = \dfrac{c_t}{c_r}$

θ(deg.)	Λ_{cr}, critical sweep angle (degrees)		
	$\lambda=0.20$	$\lambda=0.50$	$\lambda=1.0$
0	1.20	1.48	1.89
30	13.71	13.76	13.83
60	35.94	36.00	36.08
90	11.13	13.66	17.20
100	-49.08	-48.67	-48.05
120	-35.45	-35.39	-35.30
150	-13.29	-13.24	-13.16

The effect of decreasing taper ratio on Λ_{cr} is to increase Λ_{cr}, although these increases are very small. Thus, it may be concluded that taper ratio does not have a strong influence on Λ_{cr}.

Figure 9 illustrates the behavior of the divergence velocity, (normalized with respect to V_D at $\Lambda = 0$ and $\theta = 0$), as a function of θ, for $\lambda = 0.20$. Comparison of Figure 9 with Figure 7, in which $\lambda = 1.0$, shows that the sets of curves are very similar. Some differences are apparent and worth noting. In particular, near the fiber angle $\theta = 0°$, the divergence velocity at $\Lambda = 0$ declines more rapidly with θ. In addition, the curve corresponding to a sweep angle $\Lambda = -60°$ does not attain as large a maximum value when $\lambda = 0.20$ as it does when $\lambda = 1.0$. It should be noted, however, that the reference velocity is different in Figure 7 than it is in Figure 9.

29
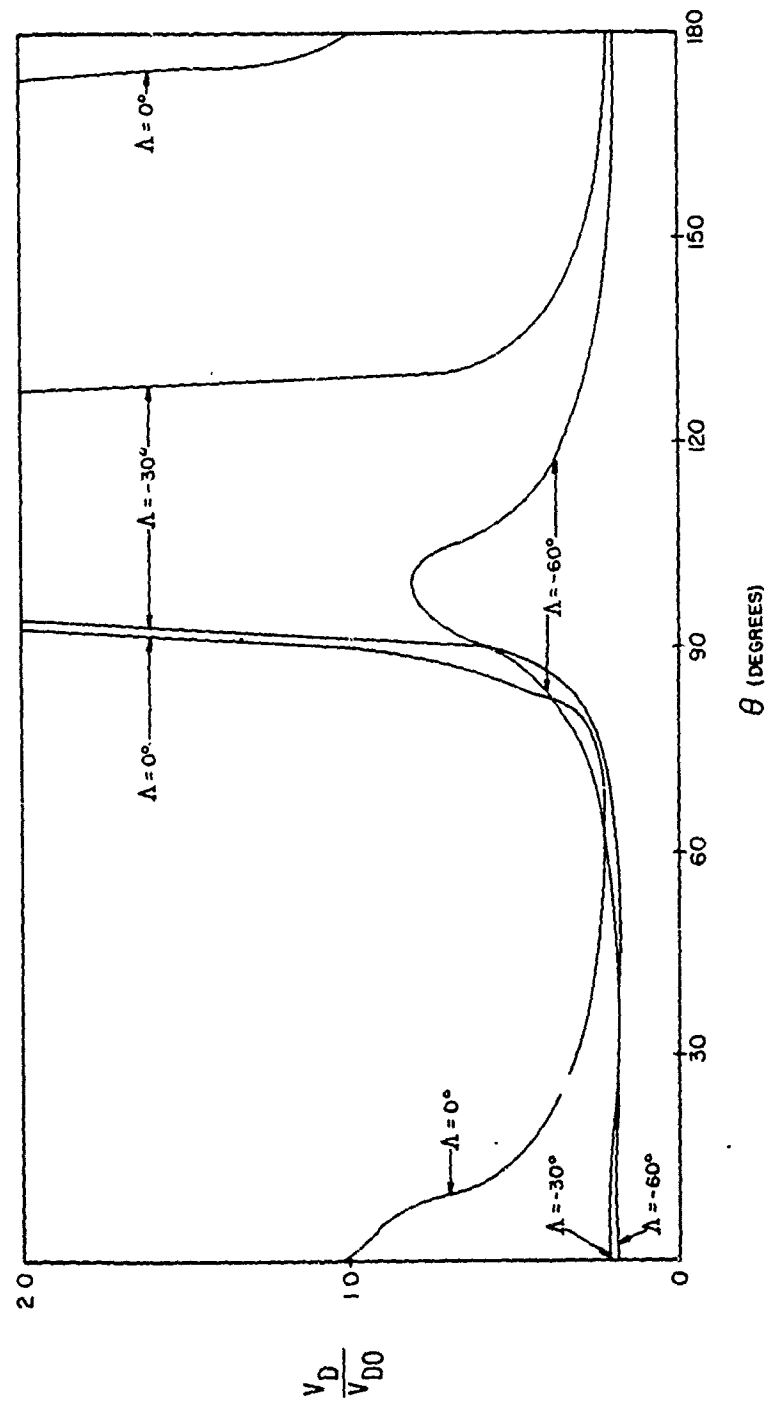
Figure 9 - Normalized divergence speed V_D/V_{DO} versus fiber angle θ for a laminate with all fibers oriented at an angle θ. Three different sweep angles; wing taper ratio, $\lambda = 0.20$; wing box to top or bottom cover sheet thickness is 20:1.

SECTION III

CONCLUSIONS

This report has presented a simple theory to predict the divergence behavior of high-aspect-ratio, laminated composite, swept wings. This theoretical development is based upon laminated beam bending theory and aerodynamic strip theory. The equations developed from this theory have been used to predict the effect of laminate construction on wing divergence. The conclusions drawn from the analysis and the example cases presented are:

1) The elastic coupling between bending and torsion, introduced by the laminated material through the parameter K, can successfully negate the undesirable influence of forward sweep on wing divergence for a wide range of forward sweep angles.

2) The ratio K/GJ is a very important parameter to consider when designing an efficient forward swept wing. This ratio should be tailored such that it has a relatively large negative value.

3) Wing taper is important to the determination of the divergence speed where such a speed actually exists. However, wing taper is of secondary importance as a parameter influencing the design of a divergence free wing.

4) The alignment of lamina fibers at angles from 10° to 15° forward of the swept wing box-beam reference axis appears to be an optimal orientation for wing divergence performance.

This report has shown that, from a theoretical standpoint, and unlike

31

its metallic counterpart, the laminated composite, forward swept wing is a feasible structural design. The formulas derived and presented in this report provide a quick, inexpensive estimation tool for further research on forward swept wing design.

APPENDIX A

THE DEVELOPMENT OF THE STRAIN ENERGY

EXPRESSION FOR A LAMINATED FILAMENTARY

WING BOX

1. BASIC ASSUMPTIONS

The wing structural model employed throughout this report is based upon the assumption that the bending stiffness and torsional stiffness of the wing structure are due entirely to the presence of relatively thin, laminated composite cover sheets, located at a large distance (in comparison to their thickness) from the wing middle surface. Although all of the bending and torsional stiffness is assumed to reside entirely in the laminated cover sheets, it would be a simple task to add algebraically any additional stiffnesses that might arise from the presence of such elements as spar caps or flexible webs.

To formulate the strain energy expression that leads to the definition of the equivalent bending stiffness, EI, and torsional stiffness, GJ, for this type of box-beam structure, it is necessary to make an assumption about the deformation behavior of the wing box. The well-known Euler-Bernoulli hypothesis that the strain due to bending varies linearly from the neutral surface of the box-beam provides this assumption about the displacement behavior of the wing. In addition, it is further hypothesized that chordwise sections of the wing, perpendicular to a beam reference axis, are rigid. This means that the deformation of the wing box is a function only of a spanwise coordinate, y. In addition to the Euler-Bernoulli hypothesis, the material behavior is assumed to be linear elastic.

33

An additional feature of the idealized beam model to be developed is that the reference surface of the box beam is taken at the geometrical middle surface of the wing box. This convention, commonly used in laminated plate theory, is more convenient than the alternative of locating a modulus weighted centroid of each section (a modulus weighted centroidal axis will always lie in the neutral surface). If the laminated box beam is not both elastically and geometrically symmetrical, the middle surface will not be the neutral surface for bending.

2. COVER SHEET DISPLACEMENTS

A Cartesian coordinate system is defined in Figure 1. The x-y plane corresponds to the geometrical middle surface of the wing box. The positive x-axis is rearward on the wing while the y-axis lies along the swept wing span and is coincident with the reference axis of the wing box. Displacements of the individual lamina forming the cover sheets are given by the functions u, v, w, in the x, y, z directions, respectively. The u, v, w displacements are not independent functions; they are functions of the variables h and α, the upward displacement of the wing elastic axis (with respect to the y-axis) and the rotation of a chordwise section about the y-axis, respectively.

In terms of $h(y)$ and $\alpha(y)$, the functions u, v, w may be expressed as:

$$u(x,y) = z\alpha(y) \tag{A-1}$$

$$v(x,y) = v_0(y) - z[\frac{dh}{dy} - x \frac{d\alpha}{dy}] \tag{A-2a}$$

or

$$v(x,y) = v_0(y) - z[h' - x\alpha'] \tag{A-2b}$$

$$w(x,y) = h(y) - x\alpha(y) \tag{A-3}$$

The variable $v_0(y)$ represents the spanwise stretching of the middle surface caused by transverse applied loads and twisting.

34

3. STRAINS IN THE COVER SHEETS

The strains in the laminated cover sheets may be determined from Equations (A-1) through (A-3). Only two strains are nonzero; these strains are:

$$\epsilon_{yy} = v'_o - z(h'' - x\alpha'') \qquad (A-4)$$

$$\gamma_{xy} = 2z\alpha' \qquad (A-5)$$

These strain-displacement expressions are seen to be consistent with the isotropic Euler-Bernoulli theory of beam bending in which there is neither transverse shear strain nor normal stress σ_z present. The strain-displacement expressions are to be used to develop the strain energy expression for the box beam, from which will result the EI and GJ expressions.

4. LAMINA CONSTITUTIVE RELATIONS

For a single orthotropic lamina, the relationship between membrane stress and strain can be written, in matrix notation, as:

$$\left\{ \begin{array}{c} \sigma_{xx} \\ \sigma_{yy} \\ \tau_{xy} \end{array} \right\} = \left[\begin{array}{ccc} \overline{Q}_{11} & \overline{Q}_{12} & \overline{Q}_{16} \\ \overline{Q}_{12} & \overline{Q}_{22} & \overline{Q}_{26} \\ \overline{Q}_{16} & \overline{Q}_{26} & \overline{Q}_{66} \end{array} \right] \left\{ \begin{array}{c} \epsilon_{xx} \\ \epsilon_{yy} \\ \gamma_{xy} \end{array} \right\} \qquad (A-6)$$

The terms $\overline{Q}_{ij}$ are functions of the orthotropic engineering constants Q_{ij} and the angle θ defining the orientation between the lamina principal axes and the wing reference axes. The lamina lies in a plane parallel to the x-y plane; the angle θ is as defined in Figure 2. The Q_{ij} terms are defined as:

$$Q_{11} = E_1/(1 - \mu_{12}\mu_{21}) \qquad (A-7)$$

35

$$Q_{12} = \mu_{12} E_2/(1 - \mu_{12} \mu_{21}) \tag{A-8a}$$

$$= \mu_{21} E_1/(1 - \mu_{21} \mu_{12}) \tag{A-8b}$$

$$Q_{22} = E_2/(1 - \mu_{12} \mu_{21}) \tag{A-9}$$

$$Q_{66} = G_{12} \tag{A-10}$$

The terms $\overline{Q}_{ij}$ can be defined in a concise manner [8] by defining a set of parameters U_i that are, in turn, functions of Q_{ij}.

$$U_1 = [3Q_{11} + 3Q_{22} + 2Q_{12} + 4Q_{66}]/8 \tag{A-11}$$

$$U_2 = [Q_{11} - Q_{22}]/2 \tag{A-12}$$

$$U_3 = [Q_{11} + Q_{22} - 2Q_{12} - 4Q_{66}]/8 \tag{A-13}$$

$$U_4 = [Q_{11} + Q_{22} + 6Q_{12} - 4Q_{66}]/8 \tag{A-14}$$

$$U_5 = [Q_{11} + Q_{22} - 2Q_{12} + 4Q_{66}]/8 \tag{A-15}$$

In terms of these new constants, the matrix terms $\overline{Q}_{ij}$ become

$$\overline{Q}_{11} = U_1 + U_2\cos2\theta + U_3\cos4\theta \tag{A-16}$$

$$\overline{Q}_{12} = U_4 - U_3\cos4\theta \tag{A-17}$$

$$\overline{Q}_{22} = U_1 - U_2\cos2\theta + U_3\cos4\theta \tag{A-18}$$

$$\overline{Q}_{16} = \frac{1}{2} U_2\sin2\theta + U_3\sin4\theta \tag{A-19}$$

$$\overline{Q}_{26} = \frac{1}{2} U_2\sin2\theta - U_3\sin4\theta \tag{A-20}$$

$$\overline{Q}_{66} = U_5 - U_3\cos4\theta \tag{A-21}$$

Note that $\overline{Q}_{16}$ and $\overline{Q}_{26}$ are antisymmetrical functions of the angle θ, while the other functions are symmetrical.

The constitutive relations for the inplane or membrane behavior of the individual lamina are used to determine the strain energy functional

36

for the box beam. In this case, the individual laminae are constrained to act as a unit because of the previously defined strain-displacement relations.

5. THE LAMINATE STRAIN ENERGY EXPRESSION

The strain energy density per unit volume for the box beam is defined as:

$$U^* = \frac{1}{2}(\sigma_{yy} \epsilon_{yy} + \tau_{xy} \gamma_{xy}) \tag{A-22}$$

In terms of this volumetric strain energy density, a functional $U(y)$ can be defined. This latter functional represents the strain energy per unit length and is expressed as:

$$U(y) = \int_{-c/2}^{c/2} \int_{-z_u}^{z_u} U^* \, dx \, dz \tag{A-23}$$

The limits of integration represent: c, the wing chord; and z_u, the z-location of the upper surface of the wing box. Symmetry, both elastic and geometric, of the wing box in the x-direction is assumed here.

The constitutive relations, Equations (A-6), can be substituted into Equation (A-23) with the following result.

$$U(y) = \frac{1}{2}\int_{-c/2}^{c/2} \int_{-z_u}^{z_u} \left[\overline{Q}_{22}^{(i)}(\epsilon_{yy})^2 + 2\overline{Q}_{26}^{(i)} \epsilon_{yy} \gamma_{xy} + \overline{Q}_{66}^{(i)}(\gamma_{xy})^2 \right] dxdz \tag{A-24}$$

The superscript (i) appended to the lamina elastic constants refers to those constants appropriate to the $(i)^{th}$ layer of the laminate.

Upon substitution of the strain-displacement expressions, Equation (A-24) becomes

37

$$U(y) = c/2 \left\{ \sum_{i=1}^{N} \left[\overline{Q}_{22}^{(i)} \beta_i (h'')^2 + \overline{Q}_{22}^{(i)} \beta_i (\frac{c^2}{12})(\alpha'')^2 - 4\overline{Q}_{26}^{(i)} \beta_i (h''\alpha'') + 4\overline{Q}_{66}^{(i)} \beta_i (\alpha')^2 \right. \right.$$

$$\left. \left. + \overline{Q}_{22}^{(i)} t_i (v_0')^2 - 2\overline{Q}_{22}^{(i)} \delta_i (v_0'h'') + 4\overline{Q}_{26}^{(i)} \delta_i (\alpha'v_0') \right] \right\} \qquad \text{(A-25)}$$

The summation in Equation (A-25) extends over the N layers of composite material. The constants β_i and δ_i are defined in terms of lamina coordinates with respect to the middle surface. In terms of the lamina thickness t_i and lamina lower and upper position coordinates z_i and z_{i+1}, respectively, β_i and δ_i are defined as follows

$$\beta_i = \int_{z_i}^{z_{i+1}} z^2 dz$$

$$= \frac{1}{3}(t_i^3 + 3t_i z_i^2 + 3z_i t_i^2) \qquad \text{(A-26)}$$

and

$$\delta_i = \int_{t_i} z \, dz$$

$$= t_i(z_{i+1} + z_i)/2 \qquad \text{(A-27)}$$

The term β_i represents the area moment of inertia of a strip of material, of thickness t_i and unit width, about the middle surface. As such, β_i is always a positive number. The term δ_i represents the first moment of the area of the same strip about the middle surface. This term δ_i is positive if the lamina area centroid lies above the middle surface and negative if it does not.

Equation (A-25) may be simplified. It is to be noted that terms containing squares of beam curvature, h", and the rate of change of twist, α', appear in this expression. Six new terms involving the laminate elastic

38

properties may be defined, leading to a more concise definition of Equation (A-25). These terms are:

$$EI_0 = c \left[\sum_{i=1}^{N} \overline{Q}_{22}^{(i)} \beta_i \right] \qquad \text{(A-28)}$$

$$GJ_0 = c \left[\sum_{i=1}^{N} 4\overline{Q}_{66}^{(i)} \beta_i \right] \qquad \text{(A-29)}$$

$$S_0 = \frac{c^3}{12} \left[\sum_{i=1}^{N} \overline{Q}_{22}^{(i)} \beta_i \right] \qquad \text{(A-30)}$$

$$K_0 = c \left[\sum_{i=1}^{N} 2\overline{Q}_{26}^{(i)} \beta_i \right] \qquad \text{(A-31)}$$

$$A_{22} = c \left[\sum_{i=1}^{N} \overline{Q}_{22}^{(i)} t_i \right] \qquad \text{(A-32)}$$

$$B_{22} = c \left[\sum_{i=1}^{N} \overline{Q}_{22}^{(i)} \delta_i \right] \qquad \text{(A-33)}$$

$$B_{33} = 2c \left[\sum_{i=1}^{N} \overline{Q}_{26}^{(i)} \delta_i \right] \qquad \text{(A-34)}$$

With these newly defined constants, $U(y)$ may be written as:

$$U(y) = \frac{1}{2}EI_0(h'')^2 + \frac{1}{2}S_0(\alpha'')^2 - K_0(h''\alpha') + \frac{1}{2}A_{22}(v_0')^2$$
$$+ B_{33}(v_0'\alpha') - B_{22}(v_0'h'') + \frac{1}{2}GJ_0(\alpha')^2 \qquad \text{(A-35)}$$

39

Equation (A-35) reveals that bending deformation and torsional deformation are coupled through the constant K_0, defined in Equation (A-31), and that additional coupling between the middle surface stretching and both bending and torsion also occurs. The terms EI_0 and GJ_0 are defined as they are because they occur in the energy terms associated with uncoupled bending and torsion, respectively.

In Reference 7, the term in the strain energy expression containing S_0 is shown to be insignificant in comparison to that term involving the term GJ_0 as long as the wing has a moderate to high aspect ratio. This term is also ignored in the analysis in the present study.

APPENDIX B

THE DEVELOPMENT OF THE COMPOSITE BEAM BENDING
AND TWISTING EQUILIBRIUM EQUATIONS FOR DIVERGENCE

1. GOVERNING EQUATIONS FOR A BEAM WITH CONSTANT CROSS-SECTION

The strain energy functional can be used, in conjunction with the Principle of Virtual Work, to derive the equilibrium equations necessary to solve the divergence problem. For the present problem, the Principle of Virtual Work can be stated as follows:

$$\delta \int_0^{\ell} U(y)dy = \int_0^{\ell} (p_y \delta v_0 + t\,\delta\alpha + p\delta h)dy \qquad (B-1)$$

The terms p_y, t and p in Equation (B-1) represent the applied generalized forces per unit length associated with the degrees of freedom v_0, α, h, respectively. These generalized forces are distributed along the length of the beam; no concentrated forces or moments are applied. For our analysis, the generalized force p_y is zero, since it represents an external axial load term.

Manipulation of Equation (B-1) yields three differential equations of equilibrium (in terms of displacement derivatives) together with the necessary boundary conditions. These differential equations are, for the constant property beam model, as follows:

$$-B_{33}\alpha'' - A_{22}v_0'' + B_{22}h''' = 0 \qquad (B-2)$$

$$-GJ_0\alpha'' - B_{33}v_0'' + K_0 h''' = t(y) \qquad (B-3)$$

$$EI_0 h^{iv} - K_0\alpha''' - B_{22}v_0''' = p(y) \qquad (B-4)$$

The boundary conditions at $y = 0$ are as follows:

41

$$v_o(0) = 0 \tag{B-5}$$

$$h(0) = h'(0) = 0 \tag{B-6,7}$$

$$\alpha(0) = 0 \tag{B-8}$$

At $y = \ell$, the boundary conditions are:

$$GJ_o\alpha' + B_{33}v_o' - K_oh'' = 0 \tag{B-9}$$

$$B_{33}\alpha' + A_{22}v_o' - B_{22}h'' = 0 \tag{B-10}$$

$$EI_oh'' - K_o\alpha' - B_{22}v_o' = 0 \tag{B-11}$$

$$EI_oh''' - K_o\alpha'' - B_{22}v_o'' = 0 \tag{B-12}$$

An understanding of the physical significance of the equations of equilibrium can be found by formulating expressions for internal force and moment resultants in terms of the displacement derivatives. Let P_y represent the internal resultant axial force present in the beam. This force resultant is defined as:

$$P_y = \iint\limits_{Area} \sigma_{yy}dxdz = A_{22}v_o' - B_{22}h'' + B_{33}\alpha' \tag{B-13}$$

The internal bending moment M_x is defined as:

$$M_x = -\iint\limits_{Area} \sigma_{yy}zdxdz$$

$$= -B_{22}v_o' + EI_oh'' - K_o\alpha' \tag{B-14}$$

From static equilibrium of an infinitesimal beam section, the internal shear force resultant V_z is given by the equation

$$V_z = \frac{dM_x}{dy} = -B_{22}v_o'' + EI_oh''' - K_o\alpha'' \tag{B-15}$$

42

Finally, the internal torque T is defined as:

$$T = \iint\limits_{Area} (z\tau_{xy} - x\tau_{xz})dxdz$$

(B-16)

$$= GJ_o\alpha' + B_{33}v_o' - K_oh''$$

Comparison of Equation (B-13) with Equation (B-2) shows that the latter equation may be written as:

$$\frac{dP_y}{dy} = 0$$

(B-17)

Since there is no loading in the axial direction, Equation (B-17) can be integrated once to produce the following result.

$$P_y = 0 = A_{22}v_o' - B_{22}h'' + B_{33}\alpha'$$

(B-18)

Equation (B-18) may be solved for v_o'

$$v_o' = \frac{B_{22}}{A_{22}} h'' - \frac{B_{33}}{A_{22}} \alpha'$$

(B-19)

Equation (B-19) may be differentiated to obtain identities for higher order derivatives of v_o, h and α. The identities obtained by differentiating Equation (B-19) may be substituted into the equation for bending, Equation (B-4) and the equation for torsion, Equation (B-3). The following equations result.

$$\left[EI_o - \frac{(B_{22})^2}{A_{22}} \right] h^{iv} - \left[K_o - \frac{B_{22}B_{33}}{A_{22}} \right] \alpha''' = p(y)$$

(B-20)

$$-\left[K_o - \frac{B_{22}B_{33}}{A_{22}} \right] h''' + \left[GJ_o - \frac{(B_{33})^2}{A_{22}} \right] \alpha'' = -t(y)$$

(B-21)

43

These equations are independent of the middle surface stretching term v_0. The boundary conditions for the problem may also be modified so that derivatives of v_0 are eliminated.

Definitions of reduced bending stiffness, EI, torsional stiffness, GI, and the coupling parameter K are readily available from Equations (B-20) and (B-21). With these definitions, Equations (B-20) and (B-21) become:

$$EI\, h^{iv} - K\, \alpha''' = p(y) \tag{B-22}$$

$$-K\, h''' + GJ\alpha'' = -t(y) \tag{B-23}$$

Boundary conditions for these equations are as follows:

at $y = 0$, $\alpha(0) = 0$ (B-24)

$h(0) = h'(0) = 0$ (B-25)

at $y = \ell$, $GJ\alpha' - K\, h'' = T(\ell) = 0$ (B-26)

$EI\, h'' - K\, \alpha' = M_x(\ell) = 0$ (B-27)

$EI\, h''' - K\, \alpha'' = V_z(\ell) = 0$ (B-28)

2. GOVERNING EQUATIONS FOR A BEAM WITH A NON-UNIFORM CROSS-SECTION

The Principle of Virtual Work also can be used to derive the governing equations for a nonuniform beam. However, an alternative way to derive these equations is to use the definitions of the bending moment, twisting moment and resultant shear force, in terms of the deformations h, α and v_0, derived in the previous section.

Once again the axial force equation yields a relationship identical to that given in Equation (B-19). The bending equation reads

$$(-B_{22}v_0' + EI_0 h'' - K_0 \alpha')'' = p(y) \tag{B-29}$$

while the torsion equation becomes

$$(B_{33}v_0' - K_0 h'' + GJ_0 \alpha')' = -t(y) \tag{B-30}$$

44

Elimination of the axial stretching term, v_o, results in two equations involving only two variables, h and α. These equations are:

$$[EI\ h'' - K\ \alpha']'' = p(y) \qquad (B\text{-}31)$$

$$[-K\ h'' + GJ\ \alpha']' = -t(y) \qquad (B\text{-}32)$$

The definitions of the terms EI, GJ, and K are identical to those discussed in the previous section. Boundary conditions for Equations (B-31) and (B-32) are:

at y = 0 $\alpha(0) = h(0) = h'(0) = 0$ (B-33,34,35)

at y = ℓ $EIh'' - K\ \alpha' = 0 = M_x(\ell)$ (B-36)

             $[EI\ h'' - K\ \alpha']' = 0 = V_z(\ell)$ (B-37)

             $GJ\ \alpha' - K\ h'' = 0 = T(\ell)$ (B-38)

3. AIRLOADS FOR THE DIVERGENCE PROBLEM

Figure 3 illustrates the geometry employed to determine the incremental lift forces and pitching moments on the swept wing. The airloads are modelled from strip theory assumptions, assumptions that tend to overestimate the aerodynamic loading and also give values for the airloads that are somewhat inaccurate at large sweep angles. Nevertheless, the value of strip theory aerodynamics lies in its ability to provide reasonably accurate aeroelastic trend information, allowing the establishment of the proper relationships between the geometric, aerodynamic and structural parameters in an aeroelastic problem.

References 1 and 9 detail the development of the use of strip theory aerodynamics for swept wing aeroelasticity problems. Of importance to the divergence problem is the determination of the incremental lift per unit of span (along the swept y-axis) arising from the deformations h and α. The reader is reminded that, for this study, h and α represent the perturbation deformations away from some slightly deformed static equilibrium position.

45

The lift per unit span due to these deformations is given by the expression

$$p(y) = (c a_0 q \cos^2 \Lambda) (\alpha - h' \tan \Lambda) \qquad \text{(B-39)}$$

While the pitching moment about the y-axis is written as:

$$t(y) = (q c a_0 e \cos^2 \Lambda) (\alpha - h' \tan \Lambda) \qquad \text{(B-40)}$$

where a_0 = lift curve slope (two-dimensional).

   c = chordwise dimension perpendicular to the y-axis.

   e = the distance between the line of aerodynamic centers (A.C.)

      and the y-axis, measured positive aft from the A.C.

   Λ = the sweep angle of the reference axis, positive rearward.

4. NONDIMENSIONALIZED GOVERNING EQUATIONS FOR A UNIFORM WING

   With the inclusion of the airloads given in Section B3, the coupled
equations governing divergence of a uniform cross-section, composite swept
wing are:

$$EI \, h^{iv} - K \alpha''' = (c a_0 q \cos^2 \Lambda)(\alpha - h' \tan \Lambda) \qquad \text{(B-41)}$$

and

$$GJ \, \alpha'' - K \, h''' = -(q c a_0 e \cos^2 \Lambda)(\alpha - h' \tan \Lambda) \qquad \text{(B-42)}$$

These equations may be written conveniently in nondimensional form. To
accomplish this, new variables are defined as follows:

$$\eta = y/\ell \qquad \text{(B-43)}$$

$$w = h/\ell \qquad \text{(B-44)}$$

$$\Gamma = dw/d\eta = dh/dy \qquad \text{(B-45)}$$

These definitions lead to the following nondimensional, coupled equilibrium
equations.

$$\Gamma''' - k \, \alpha''' = a(\alpha - \Gamma \tan \Lambda) \qquad \text{(B-46)}$$

$$\alpha'' - g \Gamma'' = -b(\alpha - \Gamma \tan \Lambda) \qquad \text{(B-47)}$$

46

where $(\ )' = d(\ )/d_{\eta}$. The boundary conditions for these equations are written as follows:

$$\Gamma(0) = 0 \tag{B-48}$$

$$\alpha(0) = 0 \tag{B-49}$$

$$\Gamma'(1) - k\alpha'(1) = 0 \tag{B-50}$$

$$\alpha'(1) - g\Gamma'(1) = 0 \tag{B-51}$$

$$\Gamma''(1) - k\alpha''(1) = 0 \tag{B-52}$$

The nondimensional parameters that appear in Equations (B-46) through (B-52) are defined as follows:

$$a = qc\ell^3 a_0 \cos^2 \Lambda / EI \tag{B-53}$$

$$b = qc\ell^2 a_0 e \cos^2 \Lambda / GJ \tag{B-54}$$

$$k = K/EI \tag{B-55}$$

$$g = K/GJ \tag{B-56}$$

5. NONDIMENSIONAL EQUILIBRIUM EQUATIONS FOR A TAPERED WING PLANFORM

A wing whose chord is linearly tapered along the wing span and whose cross-sectional dimensions are proportional to the local chord will have bending stiffness and torsional stiffness distributions that vary as the fourth power of the chord; the coupling parameter K will also vary as the fourth power of the chord. To begin the development of the equilibrium equations applicable to this problem, let us define the following terms:

$$c = fc_{root} = fc_r \tag{B-57}$$

where
$$f = 1 - \eta(1 - \lambda) \tag{B-58}$$

and
$$\lambda = c_{tip}/c_{root} = c_t/c_r = \text{wing taper ratio} \tag{B-59}$$

The subscript notation $(\ )_r$ refers to values evaluated at the wing root, while $\eta = y/\ell$.

47

Since the chord varies linearly with η and all wing sections are geometrically similar, the following stiffness parameter relationships result.

$$EI = f^4 EI_r \qquad (B-60)$$

$$GJ = f^4 GJ_r \qquad (B-61)$$

$$K = f^4 K_r \qquad (B-62)$$

Equations (B-31) and (B-32) govern the static equilibrium of the nonuniform wing and can be combined with Equations (B-39) and (B-40) (note that, in the latter two equations, $c = fc_1$) to yield an equation that is a function of the nondimensional independent variable η. The variable $f = 1 - \eta(1 - \lambda)$ also can be chosen as the independent variable. Since the latter choice of an independent offers substantial mathematical advantages when attempting a closed form solution to the problem, f, not η, is chosen as the independent variable. With f as the independent variable, the bending equation reads (note that $( )' = d( )/df$ below):

$$f^3[\Gamma''' - k_r\alpha'''] + 8f^2[\Gamma'' - k_r\alpha''] + 12f[\Gamma' - k_r\alpha'] - d_T\Gamma + \frac{d_T\alpha}{\tan\Lambda} = 0 \qquad (B-63)$$

where

$$d_T = \frac{qc_r \ell^3 a_0 \sin\Lambda \cos\Lambda}{EI_r(1 - \lambda)^3} \qquad (B-64)$$

The torsion equation becomes

$$f^2[\alpha'' - g_r\Gamma''] + 4f[\alpha' - g_r\Gamma'] + a_T[\alpha - \Gamma\tan\Lambda] = 0 \qquad (B-65)$$

where

$$a_T = \frac{qc_r e_r \ell^2 a_0 \cos^2\Lambda}{GJ_r(1 - \lambda)^2} \qquad (B-66)$$

Boundary conditions at $f = 1$ $(\eta = 0)$ are,

$$\alpha(1) = 0 \qquad (B-67)$$

$$\Gamma(1) = 0 \qquad (B-68)$$

48

while, at $f = \lambda$ $(\eta = 1)$,

$$M(\lambda) = \Gamma'(\lambda) - k_r\alpha'(\lambda) = 0 \qquad\qquad (B-69)$$

$$V(\lambda) = 4\lambda^3(\Gamma'(\lambda) - k_r\alpha'(\lambda)) + \lambda^4(\Gamma''(\lambda) - k_r\alpha''(\lambda)) = 0 \qquad (B-70)$$

$$T(\lambda) = \alpha'(\lambda) - g\Gamma'(\lambda) = 0 \qquad\qquad (B-71)$$

While these latter equations and boundary conditions now appear rather complex, they can be reduced to a form in which they can be readily solved. This simplification and solution is discussed in Appendix C.

APPENDIX C

SOLUTION OF THE WING DIVERGENCE EQUATIONS FOR CONSTANT

CHORD AND LINEARLY TAPERED WINGS

1. SOLUTION FOR CONSTANT CHORD WINGS

In Section B4, two coupled differential equations, Equations (B-46) and (B-47), were developed; these equations govern the divergence of a swept wing with a constant chord. The solution of these equations, subject to boundary conditions, Equations (B-48) through (B-52), is detailed in this appendix.

Let us begin by defining two new dependent variables, $\phi(\eta)$ and $\psi(\eta)$, to be used to transform Equations (B-46) and (B-47) into a single equation in terms of the variable $\alpha_e = \alpha - \Gamma \tan\Lambda$. In terms of ϕ and ψ, the variables Γ and α are defined as:

$$\Gamma = \phi(\eta) + k\psi(\eta) \tag{C-1}$$

$$\alpha = \psi(\eta) + g\phi(\eta) \tag{C-2}$$

where the constants k and g have been previously defined. Substitution of Equations (C-1) and (C-2) into Equations (B-46) and (B-47) yields the following:

$$\phi''' - [\frac{a}{1 - kg}][(1 - k \tan\Lambda)\psi + (g - \tan\Lambda)\phi] = 0 \tag{C-3}$$

$$\psi'' + [\frac{b}{1 - kg}][(1 - k \tan\Lambda)\psi + (g - \tan\Lambda)\phi] = 0 \tag{C-4}$$

Substitution of expressions for $\phi(\eta)$ and $\psi(\eta)$, as functions of Γ and α, obtained from inverting Equations (C-1) and (C-2), into the expression contained within the second set of brackets in both Equations (C-3) and (C-4) gives the following result.

50

$$(1 - k \tan\Lambda)\psi + (g - \tan\Lambda)\phi = \alpha - \Gamma \tan\Lambda \qquad \text{(C-5)}$$

The variable, α_e, is defined as

$$\alpha_e = \alpha - \Gamma \tan\Lambda \qquad \text{(C-6)}$$

The term α_e is the local wing angle of attack, perpendicular to the elastic axis, due to wing bending and torsional deformation. Equations (C-3) and (C-4) now read

$$\phi''' - [\frac{a}{(1 - kg)}] [\alpha_e] = 0 \qquad \text{(C-7)}$$

$$\psi'' + [\frac{b}{(1 - kg)}] [\alpha_e] = 0 \qquad \text{(C-8)}$$

If we first differentiate Equation (C-8), multiply it by the factor $(1 - k \tan\Lambda)$ and then add the result to the product of Equation (C-7) times the factor $(g - \tan\Lambda)$, the result is a single equation, written as:

$$\alpha_e''' + \left[\frac{b(1 - k \tan\Lambda)}{(1 - kg)}\right] \alpha_e' - \left[\frac{a(g - \tan\Lambda)}{(1 - kg)}\right] \alpha_e = 0 \qquad \text{(C-9)}$$

Equation (C-9) is a third order differential equation with constant coefficients.

Boundary conditions, in terms of the variable α_e, are constructed in the following manner. Equations (B-48) and (B-49) can be combined to give the equation

$$\alpha(0) - \Gamma(0) \tan\Lambda = \alpha_e(0) = 0 \qquad \text{(C-10)}$$

An examination of Equations (B-50) and (B-51) shows that both $\alpha'(1)$ and $\Gamma'(1)$ must be zero, thus, the following boundary condition results.

$$\alpha'(1) - \Gamma'(1) \tan\Lambda = \alpha_e'(1) = 0 \qquad \text{(C-11)}$$

Next, Equation (B-47) is evaluated at $\eta = 1$, multiplied by the factor $(1 - k \tan\Lambda)$, and then added to the result of the product of Equation (B-52) and the factor $(g - \tan\Lambda)$. This operation provides the third boundary condition, Equation (C-12).

51

$$\alpha_e'' (1) + [\frac{b(1 - k \tan\Lambda)}{1 - kg}]\alpha_e(1) = 0 \qquad (C\text{-}12)$$

Equations (C-9) through (C-12) constitute an eigenvalue problem. The solution to Equation (C-9) is of the form

$$\alpha_e = Ce^{r\eta} \qquad (C\text{-}13)$$

Substitution of Equation (C-13) into Equation (C-9) yields a characteristic equation whose solution provides three values for the coefficient r. This equation is

$$r^3 + \bar{a}r + \bar{d} = 0 \qquad (C\text{-}14)$$

where the constants $\bar{a}$ and $\bar{d}$ are defined as:

$$\bar{a} = \left[\frac{1 - k \tan\Lambda}{1 - kg}\right]\left[\frac{qce\ell^2 a_o\cos^2\Lambda}{GJ}\right] \qquad (C\text{-}15)$$

$$\bar{d} = \left[\frac{\tan\Lambda - g}{1 - kg}\right]\left[\frac{qc\ell^3 a_o\cos^2\Lambda}{EI}\right] \qquad (C\text{-}16)$$

Once the three roots of Equation (C-14) are determined as functions of $\bar{a}$ and $\bar{d}$, Equation (C-13) may be used to construct the stability determinant stemming from enforcement of the homogenous boundary conditions for the problem. The solution of the stability problem is accomplished by finding values of $\bar{a}$ and $\bar{d}$ which render this stability determinant zero. These critical values of $\bar{a}$ and $\bar{d}$ are denoted as $\bar{a}_D$ and $\bar{d}_D$, respectively.

The numerical solution to the stability problem itself is lengthy. Fortunately, Reference 1 details the solution to an identical set of equations. Although the problem in Reference 1 involves a metallic wing, the solution presented in Reference 1 can be adapted to the composite wing by a suitable change in the definition of appropriate constants. An approximate solution is given in Reference 1 and discussed in Section 2.4 of the present report.

52

This approximate solution is as follows:

$$\bar{a}_D = 2.47 + 0.390\bar{d}_D \tag{C-17}$$

From Equation (C-17), the value of q_D, the dynamic pressure at wing divergence, is found to be

$$q_D = \left[\frac{2.47 \ (1 - kg)}{c\ell^3 a_o \cos^2\Lambda}\right] \left[\frac{EI}{\frac{1 - k \tan\Lambda}{(\frac{\ell}{e}) \ (\frac{GJ}{EI})} - 0.39(\tan\Lambda - g)}\right] \tag{C-18}$$

2. SOLUTION FOR LINEARLY TAPERED WINGS

In Section 5 of Appendix B, the governing equations for a wing with linear taper are presented. The solution to these equations is detailed in this section. Equations (B-63) and (B-65) may be combined in a manner similar to that outlined in Section 1 of Appendix C. The procedure is as follows. First, the two variables ϕ and ψ are defined. These new variables are defined as follows:

$$\Gamma = \phi(\eta) + k_r\psi(\eta) \tag{C-19}$$

$$\alpha = \psi(\eta) + g_r\phi(\eta) \tag{C-20}$$

In addition, we define, as in the case of the constant chord wing,

$$\alpha_e = \alpha - \Gamma \tan\Lambda \tag{C-21}$$

with the definitions contained in Equations (C-19) through (C-21) and with $(\ )' = d(\ )/df$, Equation (B-63) becomes

$$f^3\phi''' + 8f^2\phi'' + 12f\phi' + \frac{d_T\alpha_e}{(1 - k_r g_r)\tan\Lambda} = 0 \tag{C-22}$$

Similarly, Equation (B-65) becomes

$$f^2\psi'' + 4f\psi' + \frac{a_T\alpha_e}{1 - k_r g_r} = 0 \tag{C-23}$$

The following procedure results in the reduction of Equations (C-22) and (C-23) to a single equation in terms of α_e:

1) Multiply Equation (C-22) by $(g_r - \tan\Lambda)$.

2) Differentiate Equation (C-23) once with respect to f and multiply the result by the quantity $f(1 - k_r \tan\Lambda)$.

3) Add the results from (1) and (2) together.

4) Make use of identities to reduce the equation resulting from (3) to the form

$$f^3 \alpha_e''' + 8f^2 \alpha_e'' + (12 + \bar{a}_T)f\alpha_e' + (2\bar{a}_T - \bar{d}_T)\alpha_e = 0 \qquad (C-24)$$

where

$$\bar{a}_T = \left[\frac{1 - k_r \tan\Lambda}{1 - k_r g_r}\right] \left[\frac{qe_r c_r \ell^2 a_0 \cos^2\Lambda}{GJ_r(1 - \lambda)^2}\right] \qquad (C-25)$$

$$\bar{d}_T = \left[\frac{\tan\Lambda - g_r}{1 - k_r g_r}\right] \left[\frac{qc_r \ell^3 a_0 \cos^2\Lambda}{EI_r(1 - \lambda)^3}\right] \qquad (C-26)$$

The boundary condition at f = 1 (the wing root) is:

$$\alpha_e(1) = 0 \qquad (C-27)$$

while, at $f = \lambda$, the wing tip, the bending moment and torque conditions, $M(\lambda) = 0$ and $T(\lambda) = 0$, give

$$\alpha_e'(\lambda) = 0 \qquad (C-28)$$

The condition of zero shear at the wing tip, when combined with Equation (B-65), evaluated at $f = \lambda$, yields

$$\lambda^2 \alpha_e''(\lambda) + \bar{a}_T \alpha_e(\lambda) = 0 \qquad (C-29)$$

The solution to Equation (C-24) subject to the boundary conditions outlined above follows that described in Reference 1 for a metallic tapered wing.

54

Reference 1 presents an approximate linear relationship between the critical value of dynamic pressure, q_D, and the geometric, aerodynamic and structural parameters in the tapered wing problem. This solution, when modified to fit the composite wing problem, provides the following equation.

$$q_D = \left[\frac{GJ_r}{a_0 c_r \ell^3 \cos^2 \Lambda}\right] \left(\frac{\ell}{e_r}\right) \left[\frac{K_1(1 - k_r g_r)}{1 - k_r \tan\Lambda - K_2 \left(\frac{GJ_r}{EI_r}\right)\left(\frac{\ell}{e_r}\right)(\tan\Lambda - g_r)}\right] \quad (C\text{-}30)$$

The constants K_1 and K_2 are functions of the wing taper ratio λ. These constants were calculated for this study and are tabulated below for four taper ratios. The values given here differ slightly from those found in Reference 1. The reason for this slight difference is probably due to the improved accuracy available today on modern computers.

λ	K_1	K_2
0.20	2.83	0.614
0.50	2.73	0.497
1.00	2.47	0.390
1.50	2.22	0.326

3. CORRECTION OF AERODYNAMIC LOADS FOR ASPECT RATIO AND SWEEP

In Reference 1, a correction for the effects of aspect ratio and sweep is suggested. This formula is

$$c_{\ell\alpha} = a_0[AR/(AR + 4\cos\Lambda)] \quad (C\text{-}31)$$

where a_0 is the 2-D lift coefficient for the unswept wing section. This correction may be used in Equation (C-18) and in Equation (C-30) in place of a_0. This correction is used throughout this report for all examples presented.

REFERENCES

1. F. W. Diederich and B. Budiansky, "Divergence of Swept Wings," NACA TN 1680, August 1948.

2. M. Knight and R. W. Noyes, "Span Load Distribution as a Factor in Stability in Roll," NACA Report No. 393, 1931.

3. R. T. Jones, "Notes on the Stability and Control of Tailless Airplanes," NACA TN 837, December, 1941.

4. S. Holzbaur, "Sweptforward Wings," Interavia, Volume V, No. 7, 1950, pp. 380-382.

5. Jane's All the World's Aircraft, McGraw-Hill Book Company, New York, 1970-71, pp. 105-106.

6. N. J. Krone, Jr., "Divergence Elimination with Advanced Composites," AIAA Paper No. 75-1009, 1975.

7. J. M. Housner and M. Stein, "Flutter Analysis of Swept-wing Subsonic Aircraft with Parameter Studies of Composite Wings," NASA TN D-7539, September 1974.

8. R. M. Jones, Mechanics of Composite Materials, McGraw-Hill Book Co., 1975, pp. 45-59.

9. R. L. Bisplinghoff, H. Ashley and R. L. Halfman, Aeroelasticity, Addison-Wesley, pp. 474-489, 1955.

10. R. L. Bisplinghoff, H. Ashley, Principles of Aeroelasticity, Dover Publications, 1975.